7e No. 4. pp. 97-128 APRIL 1942

Philips Technical Review

DEALING WITH TECHNICAL PROBLEMS
RELATING TO THE PRODUCTS, PROCESSES AND INVESTIGATIONS OF
N.V. PHILIPS' GLOEILAMPENFABRIEKEN
EDITED BY THE RESEARCH LABORATORY OF N.V. PHILIPS' GLOEILAMPENFABRIEKEN, EINDHOVEN, HOLLAND

EFFICIENCIES OF LIGHTING INSTALLATIONS

by H. ZIJL.

535.241:628.93

The empirical efficiency tables for lighting installations compiled by Harrison and Anderson more than twenty years ago are subjected to a critical examination. It is found that these fundamental empirical data can no longer be used directly for high-ceilinged rooms because of the present day use of a larger number of light points. Futhermore the examination shows that the data included in the tables probably give somewhat too low values for the illumination efficiency in the case of indirect lighting. Considering these discrepancies it may be desirable to repeat the measurements of Harrison and Anderson with modern apparatus.

The majority of the problems which arise in applied lighting technology relate to the determination of the light flux necessary to obtain a pleasing average illumination intensity E on the working surface in given circumstances. This working surface is a horizontal plane assumed to be at table height and having the same area S as the floor of the room to be illuminated. The ratio of the "effective light flux", *i.e.* the light flux which falls upon the working surface, to the nominal light flux Φ installed is called the efficiency η of the lighting installation

$$\eta = ES : \Phi \quad . \; . \; . \; . \; . \; . \; . \; . \; . \quad (1)$$

This lighting efficiency depends upon the lighting system installed, upon the proportions of the room (the ratio of length to breadth to height) and upon the reflective properties of the surfaces bounding the illuminated space. The light flux to be installed can be calculated from the given illumination efficiency for a desired intensity of illumination. It must, however, be kept in mind that the illumination intensity obtained will decrease in the course of time. This may be ascribed to several causes : the light flux of the lamps decreases, dust is deposited on the light sources and on the reflecting or transmitting parts of the fixtures, the reflectivity of painted surfaces decreases with time. This is taken into account by means of a depreciation factor d, so that the nominal light flux to be installed is represented by:

$$\Phi = \frac{ES}{\eta d} \quad . \; . \; . \; . \; . \; . \; . \; . \; . \; . \; . \; . \quad (2)$$

It is impossible to give a fixed value for the depreciation factor; the only known quantity is the average decrease in light flux of the lamps during their lifetime. In efficiency tables therefore a value of the depreciation factor based upon normal conditions and regular upkeep is usually given. It is left to the insight and experience of the illuminating engineer to change this value according to the circumstances.

The investigations of Harrison and Anderson

More than 25 years ago Harrison and Anderson carried out fundamental investigations [1]) on the illumination efficiencies which were attained with the methods of illumination then in common use. On the basis of these measurements they compiled empirical tables [2]) which are still generally used in designing lighting installations.

Their measurements were carried out in a number of test rooms having different relations between length, breadth and height, while the reflectivity of ceiling and walls could be varied in steps from black to white. Use was made successively of naked lamps, silvered reflectors directed upwards and enamelled reflectors directed downwards. Three types of the latter were examined, namely a reflector with a "broad" light distribution with which 35 to 40 percent of the light flux emitted falls within a cone with an apex angle of twice 40°, a reflector with a "narrow" light distribution with which the proportion mentioned amounts to as much as 45 tot 50 percent, and a reflector with a light distribution lying between the other two. The last mentioned light source corresponds in the first approximation to a diffusely radiating surface element with a light distribution according to Lambert's law which emits 41.3 percent of its total light flux within the above-mentioned cone.

---

[1]) Trans. I. E. S. **11**, 67, 1916.
[2]) Trans. I. E. S. **15**, 87, 1920.

For each of the lighting systems investigated the results of the measurement were represented graphically, and from the data obtained the empirical tables were derived by determining the efficiency for each combination of conditions separately by interpolation and extrapolation. Lighting systems which do not correspond to the standard cases investigated can be dealt with by combining the results of various tables in a suitable way. For those who have little experience in this field the use of Harrison and Anderson's tables is quite difficult, and for that reason various handbooks with more or less explanatory summaries have been published.

An objection to the data obtained in this way, which was not valid when the data were collected, is that in the measurements in a room whose length and width were about one and one half times the height of the light source only one central light source was installed. At the present time in such a room, even with indirect lighting, two to four fixtures would in general be used, and a lower efficiency would probably thereby be obtained. Only in the second step of their measurements, namely in a room whose length and width were two and a half times the height of the light source, did Harrison and Anderson use four fixtures.

A second objection which must be noted is a result of the fact that in the case of certain measurements the test rooms were abnormally small in dimensions compared with the fixtures used. As a result in one of the measurements for indirect lighting the distance from reflector to ceiling amounted to only 25 cm. With such a short distance an abnormally large part of the light flux is reflected by the ceiling back into the reflector, and this light must be considered as largely lost.

The enamel reflector already mentioned, which possesses a light intensity distribution approximately according to Lambert's law, furnishes a connecting link between the results of the measurements of Harrison and Anderson and theoretical illumination engineering. Cases in which the light distribution is according to Lambert's law can be used for exact calculations. The results of these calculations can then be compared with the results of measurements obtained with the last mentioned type of reflector.

Diffusely radiating ceiling and black walls

As test room let us consider the parallelopiped with edges a, b and h sketched in *fig. 1.* The upper surface $PQRS$, with direct illumination, corresponds to the plane in which the reflectors are situated, and with indirect illumination to the ceiling of the room. The basal plane $KLMN$ is the working surface. For the case which we shall deal with first, in which the walls and the working surface are black, the working surface receives only the light which comes directly from the fixtures or is reflected by the ceiling.

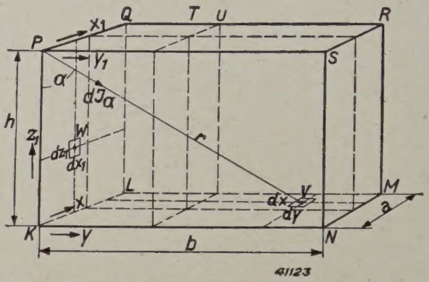

Fig. 1. Parallelopiped representing a test room. The upper surface is diffusely radiating.

If we assume that the ceiling $PQRS$ in fig. 1 is diffusely radiating with a uniform brightness, namely with a "light flux density" of F lm/m², and that the other surfaces are black, it is possible to calculate for each surface element of $PQRS$ the part e of the light flux emitted which will reach the working surface $KLMN$.

A surface element $dx_1\ dy_1$ lying in the angle P of the radiating surface possesses (since we assume diffuse radiation) a light intensity in the direction P to any given point V (x, y) on the working surface equal to

$$dI_a = \frac{F}{\pi}\cos a\ dx_1\ dy_1.$$

According to the well-known laws of illumination, the intensity of illumination at point V of the plane $KLMN$ caused by the radiating of the surface is

$$dE_V. \approx \frac{F\cos a}{\pi r^2}\cos a\ dx_1\ dy_1 = \frac{Fh^2}{\pi r^4}\ dx_1\ dy_1,$$

and the light flux which falls upon a surface element dxdy at point V, when r is expressed in terms of x, y and h, is

$$d\Phi_{P\rightarrow V} = \frac{F}{\pi}\frac{h^2}{(x^2+y^2+h^2)^2}dx_1\ dy_1\ dx\ dy.$$

By integration, once between $x=o$ and $x=a$ and then between $y=o$ and $y=b$, the expression is obtained for the light flux from the surface element at P to the whole plane $KLMN$;

$$d\Phi_{P\rightarrow KLMN} = \frac{F}{2\pi}\left[\frac{b}{\sqrt{b^2+h^2}}\tan^{-1}\frac{a}{\sqrt{b^2+h^2}}+\frac{a}{\sqrt{a^2+h^2}}\tan^{-1}\frac{b}{\sqrt{a^2+h^2}}\right]\cdot dx_1 dy_1$$

The light flux emitted by the surface element $dx_1\, dy_1$ is $d\Phi_P = F\, dx_1\, dy_1$, so that the magnitude of ε is determined by the expression within the brackets divided by 2π.

If a surface element is considered which does not lie in an angle of the radiating surface, but for instance at any point T (fig. 1) the radiating surface is divided into four rectangles which have point T in common. If the receiving surface is divided in a corresponding manner, four figures are obtained to which our formulae can be applied. The total light flux received is then related to the light flux emitted as $\varepsilon = \varepsilon_1 + \varepsilon_2 + \varepsilon_3 + \varepsilon_4$, where ε_1, ε_2, ε_3 and ε_4 indicate the proportions of each of the subdivisions of the working surface. In the case of indirect illumination the contributions to the effective light flux for the whole upper surface must be added together. The arbitrary point T thus moves over the upper surface, and the general formula for the contribution to the light flux of a surface element $dx_1\, dy_1$ at T must therefore be integrated over the whole upper surface. If the upper surface is homogeneously illuminated and if it radiates according to Lambert's law, this manipulation gives for the total light flux from the upper to the lower surface

$$\Phi_{PQRS \rightarrow KLMN} =$$

$$= \frac{2F}{\pi} ab \left[\frac{\sqrt{b^2+h^2}}{b} \tan^{-1} \frac{a}{\sqrt{b^2+h^2}} + \frac{\sqrt{a^2+h^2}}{a} \tan^{-1} \frac{b}{\sqrt{a^2+h^2}} \right.$$

$$\left. - \frac{h}{b} \tan^{-1} \frac{a}{h} - \frac{h}{a} \tan^{-1} \frac{b}{h} + \frac{1\, h^2}{2\, ab} \ln \frac{(a^2+h^2)(b^2+h^2)}{(a^2+b^2+h^2)} \right].$$

The light flux emitted by the radiating surface is $\Phi_{PQRS} = F.\ ab.$ so that division of the right-hand member of the last formula by $F.ab$ gives the ratio ε.

For the sake of simplicity we shall confine ourselves now to the discussion of the case in which the length a and the width b of the testing room are equal: $a = b$. The space ratios can then be characterized by the so-called "form index". [3])

$$K = \frac{a}{h}.$$

A small value of K thus means a high-ceilinged room, while a room which is large in proportion to its height is characterized by a large value of K.

For the ratio ε of the light flux which reaches the working surface $KLMN$ to the light flux emitted by the radiating surface $PQRS$ we now find

$$\varepsilon = \frac{4}{\pi} \left[\frac{\sqrt{1+K^2}}{K} \tan^{-1} \frac{K}{\sqrt{1+K^2}} - \frac{1}{K} \tan^{-1} K \right] + $$

$$+ \frac{1}{\pi K^2} \ln \frac{(1+K^2)^2}{1+2K^2} \quad \ldots \quad (3)$$

If K is now allowed to vary, for each element of $PQRS$ the value of ε will change with it, just as for the whole radiating surface. For four spots on $PQRS$ which are indicated in *fig. 2* by *I*, *II*, *III* and *IV*, as well as for the whole surface $PQRS$ (curve *V*) the behaviour of ε as a function of K is given in *fig. 3* for diffusely

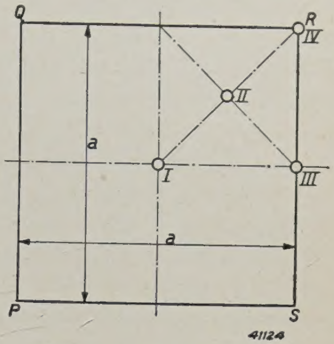

Fig. 2. Upper surface $PQRS$ of the test room with a square working surface.

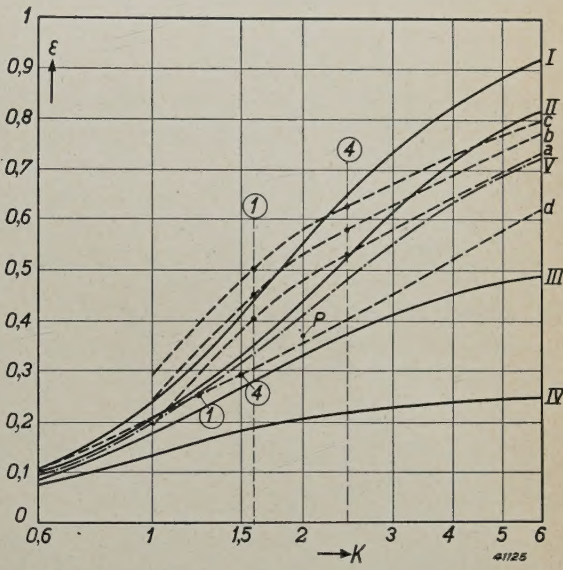

Fig. 3. The ratio ε in the case of a diffusely radiating ceiling and black walls as a function of the form index K for radiating elements lying at the points *I*, *II*, *III* and *IV* indicated in fig. 2. Curve *V* represents the behaviour of ε when the whole ceiling emits a homogeneous diffuse radiation which may be compared to an infinite number of similar sources of light. Curve *I* holds for a centrally hung light source, curve *II* for four symmetrically arranged elements. For large values of K (rooms which are large compared with their height), these two curves asymptotically approach 1, curve *III* approaches 0.5, curve *IV* approaches 0.25 and curve *V* approaches 1. Curves *a*, *b* and *c* hold for the behaviour of ε derived from the results of the measurements of Harrison and Anderson with three different types of enamel reflectors. For small values of K (high-ceilinged rooms) curve *b* follows the shape of curve *I*, which corresponds to a centrally placed source of light with light distribution according to Lambert's law. At $K = 3$ the curve takes on the form which is to be expected for four (curve *II*) and more (curve *V*) sources of light. The points indicated by *1* and *4* represent one and four light sources respectively. Curve *d* finally corresponds to indirect lighting, a loss-free reflecting ceiling being assumed.

---

[3]) This "form index" differs from the index used by Harrison and Anderson.

radiating ceiling and black walls. If we are concerned with a rectangular working surface it is found that curve V remains quite accurately valid when we assign to K the value

$$K = \frac{0.2\,a + 0.8\,b}{h} \quad \ldots\ldots\ldots\ldots \quad (4)$$

where a represents the longer side of the working surface.

It may now be expected that direct illumination with enamelled reflectors will as a rule give a curve which lies between I and V. This is indeed true to a certain extent for the reflectors investigated by Harrison and Anderson for which the curves a, b and c are derived from their tables for the limiting case of absolutely black working surface and walls. As may be expected, curve a for the reflector with a wide beam is the lowest, because with the wide light distribution the loss on the walls is greatest. Curve c of the reflector with narrow beam is the highest. The light intensity curve of the reflector giving curve b lies between the other two and most nearly approaches the form of a circle (Lambert). The irregularity in curves a, b and c may be explained by the transition from results of measurements obtained with one centrally placed source of light (values measured marked *1*) to those with four (marked *4*) and more light points.

In fig. 3 the result (curve d) is also given of the measurements of Harrison and Anderson for indirect lighting in a room with diffusely reflecting ceiling, extrapolated to a reflection factor 1 and black walls and working surface. The surface $PQRS$ is here identified with the ceiling of the test-room, while in this case also r represents the ratio between the "effective" light flux falling on the working surface and the light flux emitted by the fixtures. Theoretically a correspondence should be found between d and the calculated curve V; the irregularity of the ceiling illumination with indirect lighting with fixtures should be expressed in a higher value of ε than the one for V. However, the circumstance that part of the light flux emitted by the fixture falls directly upon the black walls ("wall loss") leads to lower values for ε.

Three conclusions may be drawn from the foregoing:

1) For direct illumination there is no reason to doubt the reliability of Harrison and Anderson's measurements. Indirect lighting, however, gave experimental results for the efficiency which are lower than expected from the theory. An explanation of this may be sought in the effect already mentioned in this article of a reflection back to the fixture, which must occur in test rooms built on too small a scale, and perhaps also in the measuring instrument used.
2) The inevitable limitation in the set-up of the investigation of Harrison and Anderson does not permit the use of the tables without previous check for lighting systems which deviate very much from the basic cases.
3) There is need of a correction of the tables based upon the present-day more lavish method of illumination for lower values of the form index K (higher rooms), for which new measurements must be made.

Diffusely reflecting walls

In the foregoing we confined ourselves to an illumination by a diffusely radiating ceiling, since we have assumed that walls and working surface were absolutely black. Actually, however, the reflections at the walls furnish an important contribution to the effective light flux, so that for an anywhere near precise calculation it is necessary to take the wall reflections into account. Since an exact calculation is impossible, attempts will be found in the literature since 1920 to reduce the method of calculation into a usable form by means of certain simplifications. None of the methods developed in this way, however, gives sufficiently reliable results. Unfortunately the measurements of Harrison and Anderson have not been repeated since 1920. Their empirical tables were, however, in 1940 supplemented by measurements of installations with tubular luminescence lamps in various types of fixtures [4]).

For completely diffusely reflecting walls it is now possible to take into account the effect of the reflections on the efficiency by considering, as was done above for the ceiling, the action of a diffusely radiating vertical wall.

For a complete calculation of the illumination efficiency in a room with reflecting walls the point of departure is the light distribution of the fixture employed. With a given arrangement of the light points it is possible to deduce from this light distribution how the surfaces which bound the room are illuminated by the direct light flux. This can be done graphically, or idealized light distributions can be chosen for the general case, which are wholly or partly susceptible to exact calculation. Such a set of light intensity curves [5]) is reproduced in *fig. 4*.

When the light flux distribution on the surfaces bounding the room has been determined and thus also the direct component of the effective light flux, the light flux is then calculated which reaches the working surface after first being reflected by the ceiling. This is possible since with given proportions of the room the value of ε can be determined for every point on the ceiling. A practical method is to divide the ceiling into a number of rectangular areas to which in good approximation the same value of ε may be assigned as for the centre of each rectangle. The light flux reflected by the ceiling which is not directed toward the working surface strikes the walls, and in addition a part of the light emitted by the fixtures is radiated directly to the walls. By introducing suitable simplifications it is possible to calculate what part of the light reflected by the wall will be directed to the working surface and what part to the other walls and to the ceiling. Of these last two contributions the part is calculated which still reaches the working surface after the repeated reflection. This contribution is then multiplied by a certain factor to account for the irregularity of the distribution of the light flux over the walls in question.

---

[4]) Trans. I. E. S. 35, 759, 1940: W. M. Potter and W. G. Darley, The design of luminaires for fluorescent lamps.

[5]) For an indirect illumination by means of a cove along the wall the calculation is somewhat more complicated.

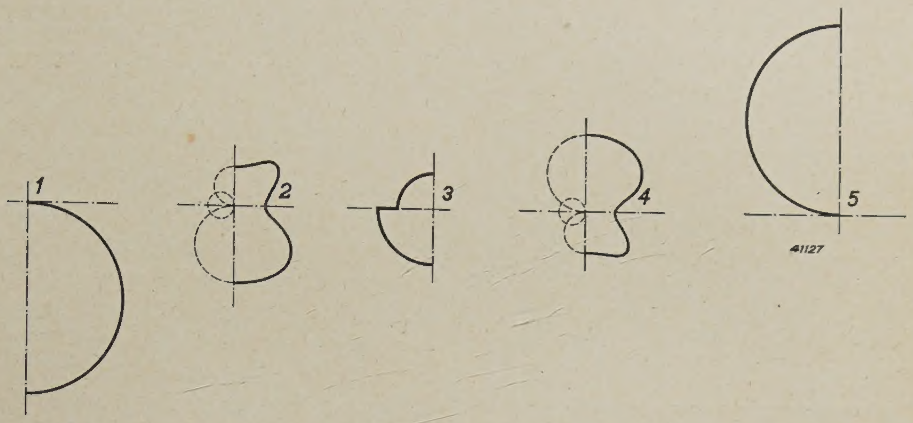

Fig. 4. Light intensity curves for five common lighting systems: 1) direct, 2) half-direct, 3) diffuser, 4) half-indirect, 5) indirect. The more complex light distributions 2) and 4) are composed of the spherical light ditributions of a direct and an indirect component, as well as the toroidal distribution of a lateral component. The five diagrams relate to the same total light flux.

In order to perform the calculations described we begin with a diffusely radiating surface element $dx_1\,dy_1$, lying at any given point $W\ (x_1,y_1)$ on the vertical plane $KLQP$ of the parallelopiped of fig. 1, and determine the light flux $d\Phi_{W\rightarrow V}$ emitted by it which falls upon the horizontal surface element $dx\ dy$ at any given point V on the working surface:

$$d\Phi_{W\rightarrow V}=\frac{F}{\pi}\left\{\frac{yz_1}{(x-x_1)^2+y^2+z_1{}^2}\right\}^2 dx_1\ dz_1\ dx\ dy.$$

When we integrate this light flux over the whole side wall $KLQP$ and over the whole working surface $KLMN$, assuming the illumination of the side wall to be homogeneous, we obtain ⁶)

$$\Phi_{KLQP\rightarrow KLMN}=$$
$$=\frac{F}{\pi}ah\left[\tan'^{1}\frac{a}{h}-\frac{\sqrt{b^2+h^2}}{b}\tan'^{1}\frac{a}{\sqrt{b^2+h^2}}+\frac{b}{h}\tan'^{1}\frac{a}{b}+\right.$$
$$+{}^1\!/\!_4\frac{b^2}{ah}\ln\frac{b^2\ (a^2+b^2+h^2)}{(a^2+b^2)(b^2+h^2)}-{}^1\!/\!_4\frac{a}{h}\ln\frac{a^2\ (a^2+b^2+h^2)}{(a^2+h^2)(a^2+b^2)}+$$
$$\left.+{}^1\!/\!_4\frac{h}{a}\ln\frac{h^2\ (a^2+b^2+h^2)}{(b^2+h^2)\ (a^2+h^2)}\right].$$

Actually the illumination of the side wall is by no means homogeneous. It is therefore desirable to divide this wall into horizontal strips and to carry out the calculation with the average value of F belonging to each separate strip. Division of the wall into strips gives sufficient accuracy.

For the calculation of the influence of the successive reflections we start for the time being with the assumption that the light fluxes concerned are entirely uniformly distributed over the areas on which they are incident. Of a light flux Φ_w which hits a wall, a fraction $R\Phi_w$ is reflected toward the ceiling as well as toward the working surface, while a fraction $W\Phi_w$ is reflected toward the other walls. Of the light flux $R\Phi_w$ falling on the ceiling a part $PR\Phi_w$ goes back again to the walls, while $QR\Phi_w$ falls upon the working surface. For the sake of simplicity we may continue to assume that the working surface is black. Due to the second reflection on the walls a light flux $PR^2\Phi_w$ is now furnished on the working surface and the same on the ceiling, while $PRW\Phi_w$ goes to the other walls.

In this way we now obtain an infinite series of light flux contributions whose sum for the total light flux furnished on the working surface by the uniformly reflecting walls is finally found to amount to:

$$\Phi_{w\longleftarrow\longrightarrow v}=\Phi_w\frac{R\ (1+Q)}{1-(PR+W)}.$$

The light flux which finally reaches the working surface from a uniformly reflecting ceiling is found in a similar way, and amounts to:

$$\Phi_{p\longleftarrow\longrightarrow v}=\Phi_p\frac{PR\ +\ Q\ (1-W)}{1\ -\ (\ PR\ +\ W)}.$$

A correction must still be applied to the part of the effective light calculated in this way. Considering the fact that the light flux distribution which occurs upon repeated reflection is not uniform, the light flux

---

⁶) This formula was already derived by Lambert, although not quite directly (Photometria, 1760).

actually falling on the working surface will deviate from that calculated. Since, however, the part in question is small compared with the rest, the great accuracy which is only to be obtained by very laborious calculation is unnecessary.

As the result of a series of calculations *fig. 5* gives four curves for an indirect illumination with fixtures. The quantity ε is again the ratio of the effective light flux to the light flux emitted by the fixtures. For each curve the reflection factor of the ceiling (ϱ_p) and of the walls (ϱ_w) is indicated. The corresponding dotted line curves, taken from the tables of Harrison and Anderson, serve for comparison. The calculated curves show, as already mentioned, higher values than those found empirically. Moreover, they are considerably steeper because they are calculated for four points of light even for low values of K. If they were calculated for a single centrally placed light point up to $K = 2$, they would up to this point also be about parallel to the empirical curves at somewhat higher values of ε.

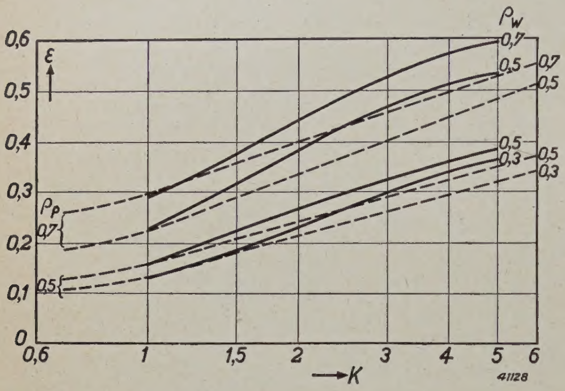

Fig. 5. The ratio ε for indirect illumination in rooms whose ceiling as well as the walls are reflecting; as in fig. 3 the form index K is plotted horizontally. The full-line curves are valid for the calculated values of ε, and the broken-line curves are derived from the tables of Harrison and Anderson. The reflection factors for ceiling and walls are indicated by ϱ_p and ϱ_w respectively.

Practical diagrams

Fig. 6 gives a completely worked out picture of the distribution of the light upon different reflections. A fixture was used with the following characteristic: 17 percent absorption in the fixture, 70 percent of the light flux emitted in the upper hemisphere and 30 percent in the lower hemisphere (see *fig. 7*). The interpretation of fig. 6 is extremely simple. On the left the reflectivity of the ceiling and of the walls is indicated. Then follows a column for the form index K for each reflection group and then the final efficiency η corresponding to every value of K. The graphs show how the light flux is distributed. Irrespective of the surroundings 17 percent of the light flux is lost by absorption in the fixture. In time this loss increases due to dust deposits. Moreover, the light flux of

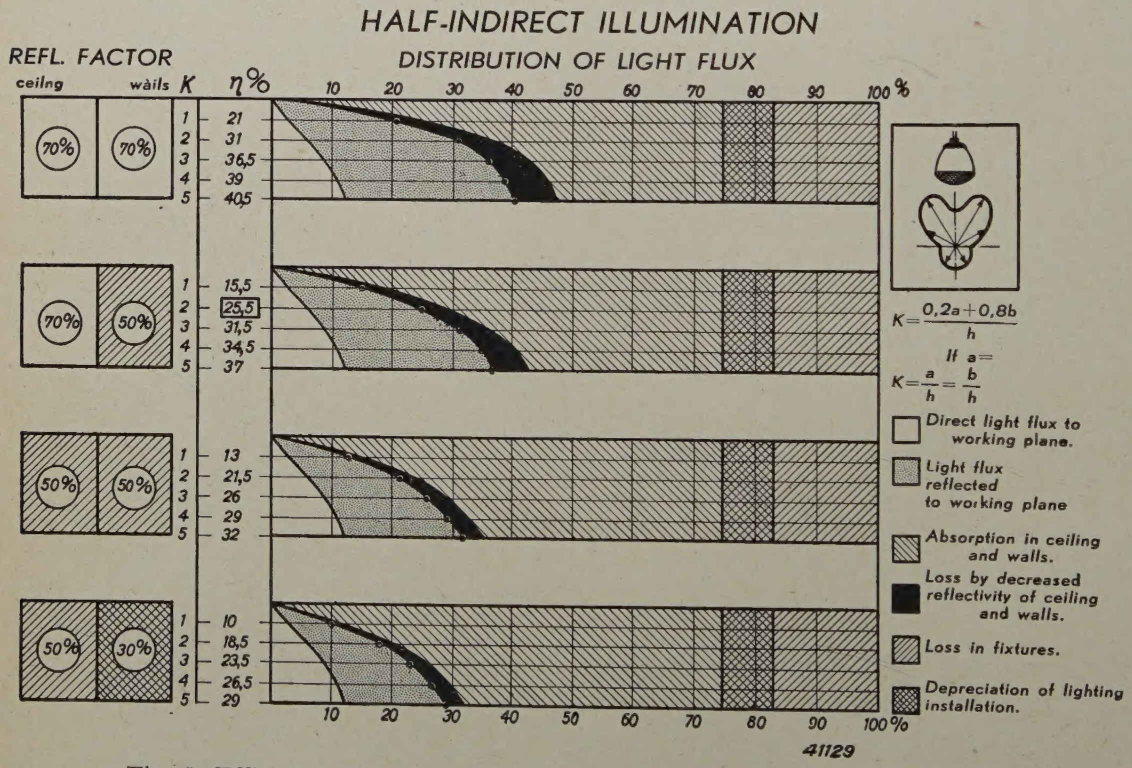

Fig. 6. Efficiency table and distribution of the light flux for a half-indirect illumination. A collection of such figures relating to average cases occurring with common lighting systems will be published in the book "Kunstlicht en Architectuur" (Artificial Illumination and Architecture) by L. C. Kalff, which will appear shortly.

the lamps decreases, so that in the ordinary case after the elapse of some time it may be expected that about 74 percent of the nominal light flux will leave the fixture. This 74 percent will be divided into the light flux which reaches the working surface directly (extreme left in the graph), the light flux which reaches the working surface after reflection on the ceiling and walls (between the left-hand and the two right-hand curves), and the light flux which is absorbed by the walls and ceiling. This last part, and with it the part before the last, changes with time, the reflecting walls become darker. If it is assumed that 70 percent reflectivity decreases by a factor 0.85, 50 percent by a factor 0.9 and 30 percent by a factor 0.95 of the original values, the transition region between the two righthand curves occurs. The two curves are calculated on the basis of 74 percent of the nominal light flux. In the beginning therefore an efficiency which amounts to 83/74 of the value indicated by the right-hand curve may be counted on. The efficiency gradually decreases to the values of the second curve from the right, which corresponds to the figures in the column beside the graph. It is evident that the parts of the effective light flux vary in the first approximation proportionally with the light flux emitted by the fixture, so that any necessary reduction offers no difficulties.

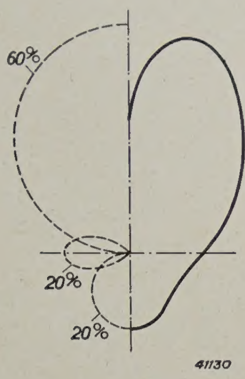

Fig. 7. Light intensity diagram for the half-indirect fixture for which the efficiency table is given in fig. 6. On the right the total light intensity diagram of the armature is drawn, while on the left the three components (direct, indirect and lateral) of which the light distribution can approximately be built up are indicated by a broken line.

From the graph it is evident that the part of the direct light flux which is independent of the ceiling and wall reflections increases absolutely as well as relatively with the form index. The diffuseness of the illumination decreases upon decrease of K. The form index K (see equation (4)) introduced by us for a diffusely radiating ceiling is found to be sufficiently accurate for other cases as well, and has the advantage of being simpler than that of Harrison and Anderson, so that there is less chance of error. The results obtained with it differ only little from those of Harrison and Anderson and also agree satisfactorily with other known experimental results.

FILTERS FOR CARRIER-WAVE TELEPHONY INSTALLATIONS

by TH. J. WEYERS. 621.318.7:621.395.44

In carrier-wave telephony, since the conversations of different subscribers, modulated on different carrier waves, must be transmitted over the same line, care must be taken that only the desired frequency bands reach each receiving channel. This means that the frequency bands of the other channels which would cause cross talk must be suppressed by filters with adequate attenuation. The requirements which must be made of the total attenuation of these filters may be deduced from the intensity distribution of the speech, the sensitivity of the microphone, telephone and human ear and the permissible degree of cross talk. This deduction is explained in this article, using as example the installation of a 17-channel system designed by Philips. A discussion is also given of the way in which the required total attenuation must be divided among the different filters at the transmitting and receiving end, while in conclusion the construction of the filters and the results obtained with them are described.

In an earlier number of this periodical [1]) an outline was given of the equipment of an installation for carrier-wave telephony. It was found that the various filters thereby perform an important function. We shall here indicate more presicely the requirements which these filters should fulfil, and study the way in which the filters are built up.

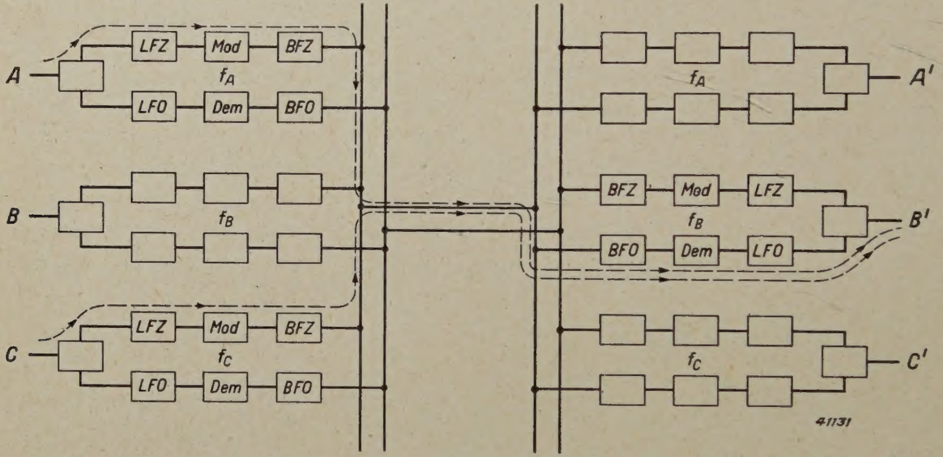

Fig. 1. Simplifed diagram of a carrier-wave telephone installation. Three channels are indicated. *LFZ* low-pass transmitting filters, *Mod* modulators, *BFZ* transmitting band-pass filters, *BFO* low-pass receiving filters. The cross talk between adjacent channels (*A* to *B'*, *C* to *B'*) is indicated by dotted lines.

Fig. 1 gives once more a simplified diagram of a carrier-wave installation for three speech channels in which *A* speaks with *A'*, *B* with *B'* and *C* with *C'*. In each speech channel, at the transmitting as well as at the receiving end, there is a low-pass filter and a band-pass filter. Let us now suppose that the two transmitting filters at *C* and the two receiving filters at *B'* are missing. In addition to the upper side band of *C*, which is cross-hatched in *fig. 2*, and which we actually wish to use for the transmission of the conversation, the lower side band is also transmitted by *C*. Futhermore the two side bands transmitted have a much greater width (indicated by the dotted line in fig. 2) than the band of about 300 to 3000 c/sec required for the transmission, since in speech itself frequencies up to above 10 000 c/sec occur. Finally

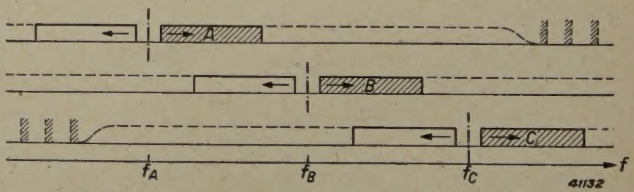

Fig. 2. Transmitted frequency spectra of the three speakers *A*, *B* and *C* in the absence of filters at the transmitting end. By the modulation of the speech spectrum on the respective carrier waves f_A, f_B and f_C, the side bands indicated are formed. Of these only the shaded portion in each case should be used for the transmission. The dotted lines with each spectrum represent the by-products of the modulation which actually, although with low intensity, also occupy whole frequency bands. The carrier waves themselves are not generally transmitted.

---

[1]) D. Goedhart and J. de Jong, Carrier-wave telephony, Philips techn. Rev. 6, 325, 1941. See also: F. A. de Groot and P. J. den Haan, Modulators for carrier-wave telephony, Philips techn. Rev. 7, 83 1942.

several kinds of weaker undesired frequency bands are also sent out by C, which are formed chiefly in the modulator and are indicated in fig. 2 by a few lines.

Due to the absence of the filters mentioned, subscriber B' receives not only the desired side band from B, but also the whole frequency spectrum sent out from C; cross talk occurs, and in this case it is unintelligible cross talk, since in the channel of B' the frequency spectrum of C is not demodulated with its original carrier wave f_C, but with the carrier wave f_B lying, for instance, 4000 c/sec lower. A speech frequency f, which by the modulation was converted into $f_C - f$ and $f_C + f$, after the "wrong" demodulation, now appears as frequency $f_C - f - f_B = 4000 - f$ or as $f_C + f - f_B = 4000 + f$. The lower side band of C is thus "inverted" for B', *i.e.* the low frequencies become high frequencies and *vice versa*. In the upper side band all the frequencies are increased by the amount $f_C - f_B$.

In the same way, when we suppose the transmitting filters of A to be absent, cross talk from A to B' occurs, but with the difference that now the upper side band of A is inverted and the lower band shifted upward. Furthermore, the more distant channels may also cause cross talk by means of the parts of the frequency spectra indicated in fig. 2 with dotted lines.

The function of the filters is now to prevent this cross talk.

It is quite clear that cross talk would be prevented if at the transmitting and receiving end of each channel band filters were introduced, each of which passed exclusively the side band belonging to that channel (shaded in fig. 2) and possessed an infinitely large attenuation on both sides of that frequency region. Such filters are impossible of realization in practice of course, and actually it is unnecessary to isolate the frequency bands so rigorously from each other, because the interference voltages always have only a finite amplitude and a certain small amount of cross talk does not prevent the carrying on of a satisfactorily intelligible conversation. For reasons of economy indeed it is desirable not to make the filters, which are made up of filter sections in series composed of coils and condensers, better than is absolutely necessary in connection with the permissible amount of cross talk. In order to design the filters for a given carrier-wave telephone installation, therefore, it is first necessary to study in detail the attenuation which each frequency must experience on the undesired path from C to B' or from A to B', etc. in order to keep the cross talk just within the permissible limits.

This must be done in different steps. For each separate frequency the following must be taken into account: the intensity of the speech to be expected at this frequency, the strength in which vibrations of this frequency are transmitted by the microphone, the sensitivity of the cross talk. By the combination of these data the desired attenuation curve is found.

In the following we shall explain more fully the steps mentioned for determining the attenuation requirements, choosing as basis the situation in the case of a 17-channel carrier-wave telephone system worked out by Philips. In this case the frequency difference of the successive carrier waves amounts to 4 kc-sec and the upper side band is transmitted, as was assumed above. In conclusion the method will then be discussed by which the attenuation curve found is given practical realisation in the filters.

The spectral distribution of the intensity of speech

It is impossible to reproduce the energy distribution of speech vibrations over all frequencies simply by a Fourier spectrum. The sounds of speech change continually and with them also the intensity of the different components in the spectrum. One may of course consider the average value of the intensity at each frequency, but this would lead to incorrect conclusions in the problem here presented. If for instance we gave the filters an attenuation curve such that at each frequency the average intensity of the interfering speech vibration was attenuated to below the threshold of hearing, then in the continual fluctuation of the intensities the peaks would still project above the threshold of hearing at times, and it is just these peaks which may cause an interference. The intensity distribution of the speech must therefore be characterized by the magnitude and the number of the peaks occurring at each frequency and the peaks may for instance be counted with a recording apparatus.

The term "each frequency" used above must still be defined more fully. If by means of a filter with an ideally sharp resonance curve a single frequency, *i.e.* an infinitesimally narrow frequency region, should be filtered out of the speech spectrum, no intensity of that frequency would ever be observed. In measuring therefore a small frequency region of a certain width must be investigated in each case, and in order to be able to record the correct size of the peak in the speech, the width must be greater than the spectral width which the peaks ordinarily possess, but still narrow enough so that in general two peaks cannot occur in it at the same time to be recorded as a single peak of a greater height.

A similar problem is encountered in connection with the time which is available for the recording of each peak. This time must be long enough so that a peak is recorded as a whole, since otherwise instead of one peak two or more are recorded. On the other hand the time for recording must also not be so long that there is danger of counting two successive peaks as one.

Considering these elements of uncertainty which lurk in the characterization of speech it is not to be wondered at that the results of different investigators are somewhat divergent in these respects. Moreover, the results, which of course are averages in each case over a number of speakers, depend to a certain extent upon the language, and, related, to this, upon the articulation of the speakers. Nevertheless, it has been found possible with the data available in the literature [2]) to construct with sufficient accuracy a generally valid basis for our considerations, a basis which, according to experiments with the filters constructed, need not be subjected to modifications for different languages.

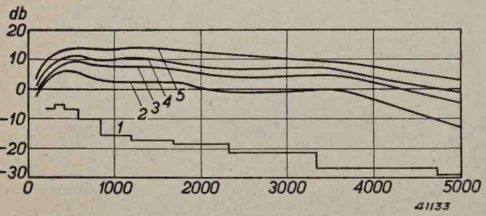

Fig. 3. Spectral distribution of the intensity of speech for an average speaker. The average over the time of the level of the whole sound is set equal to 0 db. The stepped curve *1* gives the average intensities which occur in the different frequency intervals (half an octave wide). Curves *2*, *3*, *4*, *5* give the levels which are exceeded by the intensity peaks in speech once per second, once per 3 seconds, once per 6 seconds and never, respectively.

In *fig. 3* several curves are now given which were derived from the data mentioned, and which describe the intensity distribution in speech. As a basis for the measurement, in agreement with Fletcher and others, a frequency interval of a half an octave is assumed and a time interval of 1/8 second. For each frequency interval the average intensity level (in db) occurring therein is plotted and the level which is never exceeded, exceeded once in 6 seconds, once in 3 seconds and once per second, respectively. The average intensity level of the whole conversation is set equal to 0 db. This figure thus gives a picture of the height and the number of the intensity peaks occurring in each frequency interval for an average speaker.

The sensitivity of the microphone

The sensitivity of a microphone of the kind used in telephony is closely dependent on the frequency, as is shown in *fig. 4* for two different types of microphone. The form of the microphone currents occurring as functions of the frequency thus deviates from the form of the air vibrations which are incident upon the microphone when it is spoken into. The resulting intensity distribution can be constructed in a simple way by multiplying the intensities given in fig. 3 for each of the successive frequency intervals by the average sensitivity of the microphone over this interval. Now according to fig. 4, however, the frequency characteristics of different types of microphones vary quite considerably. In the construction of an installation for carrier-wave telephony the fact must be taken into account that the subscribers may use any given type of microphone and that in spite of this cross talk should remain below the permissible limit in every case. We have therefore carried out the construction described for curve 1 of fig. 3 for several types of microphone, among which are those whose characteristics differ most widely, and have then determined the uppermost "envelope" of the curves for the different microphones. This envelope, which is drawn as curve *1* in *fig. 5*, now gives, as a function of the frequency, the level above which the average over the time of the intensity of the microphone currents does not project, no matter what type of microphone is used. Here also the average level of the total microphone current is set equal to 0 db. With the help of the other curves of fig. 3 the curves *2*, *3*, *4* and *5* in fig. 5 are then also constructed, and these indicate respectively the levels which are exceeded once per second, once per 3 seconds,

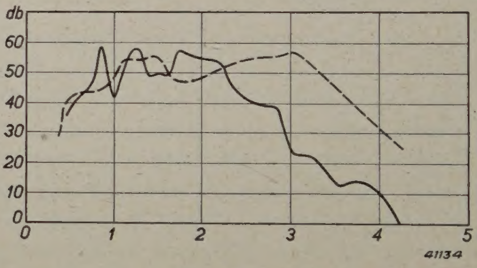

Fig. 4. Frequency characteristics of two different common types of microphones (the zero level is arbitrary).

---

[2]) See especially H. Fletcher, Physical characteristics of speech and music, Rev. mod. Phys. 3, 258, 1931. Further also publications by Crandall, Sivian, Fletcher and Munson and Colpitts in Bell System techn. J. 1925 to 1937, as well as F. Trendelenburg. Klänge und Geräusche, Springer, Berlin 1935.

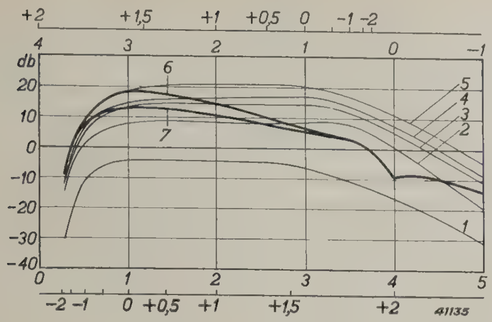

Fig. 5. Spectral distribution of the microphone currents averaged over different speakers. The average over time of the level of the whole conversation is set equal to 0 db. Curve *1* is the "envelope" of the curves found with different types of microphone for the average intensities which occur in the different frequency intervals. Curves *2*, *3*, *4*, *5* give the levels which are exceeded by the intensity peaks of the microphone currents once per second, once in 3 seconds, once in 6 seconds and never, respectively. The level which is exceeded once per 3 seconds serves as a basis for the permissible cross talk. Due to the inversion experienced by the speech spectrum upon demodulation with the "wrong" carrier wave (that of an unintended subscriber) a partial compression and partial expansion of the spectrum takes place which may be seen in the octave scale which is given for the original as well as the inverted spectrum (lower and upper scales respectively). As starting point the frequency 1000 c/sec is arbitrarily chosen. Due to this compression and expansion curve *3* must be replaced by curve *6*. The limiter present in every channel provides that the strongest peaks in the microphone currents are attenuated by about 6 db, so that curve *6* passes over into curve *7*.

once per 6 seconds and never exceeded [3]).

The permissible level of the interferences received

Which one of the curves in fig. 5 must now be used as a basis for the further discussion? We have already stated that it is unnecessary to give the filters so much damping that the conversation of *A* or *C* remains entirely below the limit of hearing of *B'*. Therefore we need not use the level curve which is never exceeded by the peaks (curve *5*). It has been found experimentally that the following of a telephone conversation is not appreciably disturbed when an interfering conversation causes an audible sound not more than once in three seconds. In the first instance therefore we begin with curve *3* in fig. 5. As this level is of course exceeded in each frequency interval of half an octave once in three seconds just as many interfering sounds would be heard every three seconds as there are half octaves in the whole frequency region. It will appear later that this is not actually the case, however, and that we may without hesitation work upon the assumption that in each half octave an audible sound may occur once in three seconds.

This condition holds for the receiving channel. Now the lower side-band of the frequency spectrum of *C* reaches the telephone of the unintended subscriber *B'* in an inverted form (see above). Thus for example the region from 300 to 1400 c/sec of the original spectrum, *i.e.* more than four half octaves, is transferred into the region from 2600 to 3700 c/sec, *i.e.* about one half octave. In order to hear an interference in the receiving channel within this single octave only once in three seconds, an audible interference must occur within the region from 300 to 1400 c/sec of the original spectrum only about once in twelve seconds per half octave, *i.e.* practically never. For corresponding reasons in the half octave from 2600-2700 c/sec of the original spectrum an audible interference may occur more than once in three seconds. In this way curve *6* of fig. 5 is found as the level of the speech currents which is exceeded as often as corresponds to the permissible interference in the receiving channel being interfered with.

What is plotted in fig. 5 is actually the difference between the peak intensities occurring and the average speech intensity. Now in every carrier-wave telephone installation so-called amplitude limiters are employed, which are placed in every channel between the microphone and the modulator and whose function is to limit the largest current maxima occurring. This precaution, which is taken mainly to combat overloading of the line repeaters, also has the result that with a given degree of cross talk larger average microphone currents can be used. It has been found experimentally that the average currents may be twice as large. For our curve this is the same as if the amplitudes of the highest peaks occurring (which cause the cross talk) were a factor 2 lower, *i.e.* as if they reached a level 6 db lower. According to curve *6* of fig. 5 the highest peaks which thus fall victims to the action of the limiter occur at about 1000 c/sec. Therefore we may allow the curve to fall about 6 db in this region and thereby finally obtain curve *7*, which now indicates the level to be considered or the permissible interference. This curve is drawn separately in *fig. 6*.

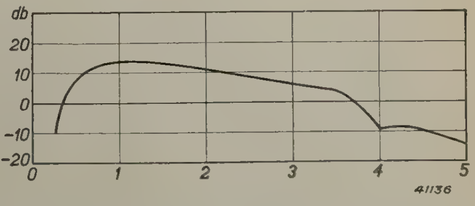

Fig. 6 Spectrum of the interferences which must be used as a basis for the damping requirements.

---

[3]) The C.C.I.F. (Comité consultatif international de communications téléphoniques à grande distance) propose a network which, as far as its frequency characteristic is concerned, may be considered as the equivalent of the microphone. We have not used this, in order to be able to take into account also the properties of better microphones which were not yet in use when the C.C.I.F. characteristic was determined.

The threshold of the disturbing effect caused by interference

The filters between C (or A) and B' serve to provide that an interference with the spectrum of fig. 6 falls just below the threshold of hearing of B', or more accurately below the threshold of the disturbing effect. In determining this threshold the sensitivity of the ear of B', as well as the sensitivity of the telephone which converts the electrical vibrations into audible air vibrations plays its part. Both sensitivities depend very closely upon the frequency, as is shown in *fig. 7*. In this figure the sensitivity of the ear (measured at the level of interference permissible for telephony) and the sensitivityof two different types of telephone are plotted, all three in db at an arbitrary zero level. In addition to these frequency characteristics of ear and telephone, various kinds of physiological effects also play a part in the disturbing effect of a sound, such as occur upon the simultaneous presence of a desired and an undesired sound. In order also to take these effects into account there is no other possible way but to determine the threshold of the disturbing effect directly by experiment. This is done in the following way. The interference voltage is measured with a voltmeter, and it has been found that the deflection observed may be considered as an objective measure of the disturbing effect independent of the nature of the interference voltage, provided the voltmeter is given a very definite frequency characteristic by means of a filter connected in series with it. Such a measuring instrument is called a psophometer, and the psophometer characteristic mentioned, in which the ear sensitivity and the sensitivity of the telephone are already taken into account, furnishes the desired threshold curve of the disturbing effect when the empirical fact is also taken into account that an interfering sound in the telephone is only just not experienced as disturbing when the psophometer indication lies 62 db below the average level of the telephone conservation.

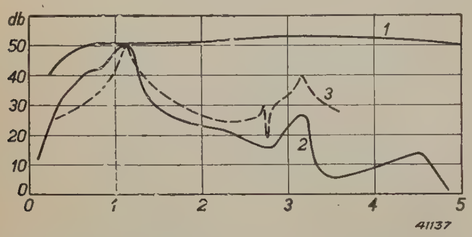

Fig. 7. Spectral sensitivity of the human ear (*1*) and frequency characteristics of two different types of telephone (*2* and *3*). The zero level is arbitrary.

The threshold curve of the disturbing effect so obtained must be recorded with different common types of telephones in order to make it possible, in the same way as described above for the microphone, to draw the "envelope" of the curves obtained for different telephones. Taking into account the possibility that the telephones now in common use may be replaced by newer and better types [4]), we have arrived at the threshold curve of the disturbing effect reproduced in *fig. 8*.

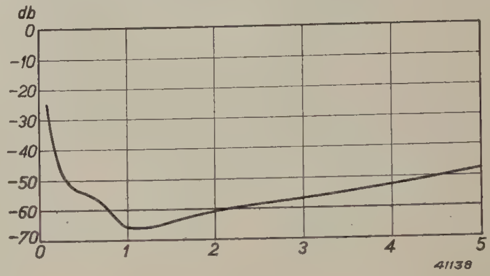

Fig. 8. Threshold curve of the disturbing effect obtained from the psophometer characteristic. At each frequency the interference must be attenuated to below the level indicated here.

The required attenuation of the filters

In order to derive the required attenuation curve of the filters from the interference curve fig. of 6 and the threshold curve of fig. 8, we must still ascertain what takes place in modulation and demodulation. The interference with the spectrum according to fig. 6 is for instance modulated on the carrier wave f_A. The side bands on both sides of f_A indicated in *fig. 9* by the two branches of curve *1* are thereby formed. If we assume further that B' receives a sound which has at all frequencies exactly the intensity of the threshold curve according to fig. 8, this sound can occur by demodulation not only from the right-hand but also from the left-hand side band of the carrier wave f_B. In the frequency regions of the demodulated vibrations, therefore, the threshold curve *2* drawn in fig. 9, consisting of two branches to the right and left of f_B, must be taken into account. The difference between curves *1* and *2* gives the curve of the required total attenuation of the filters between A and B' (curve *3*).

In this curve is included not only the contribution of the band-pass filters but also that of the low-pass filters. The actual attenuation curves of the latter lie, of course, in the audio-frequency region and must therefore, like the curves of fig. 6 and fig. 8, be considered to be transferred by modulation on the carrier-waves

---

[4]) The C.C.I.F. also gives a psophometer characteristic in which, however, the use of modern telephones is not yet taken into account.

f_A and f_B, respectively, to the frequency region of the modulated vibrations considered in fig. 9, in order to be able to add them to the attenuation of the band-pass filters.

If we do not consider the cross talk from A to B' (to the higher channel), but from C to B' (thus to the lower channel), it is easy to see that the required attenuation is represented by a curve symmetrical to curve *3* of fig. *9* with respect to f_B.

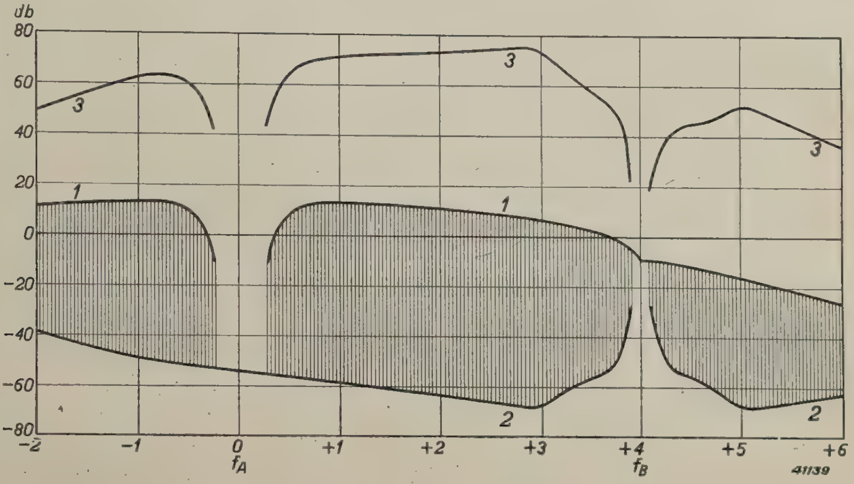

Fig. 9 In the frequency region of the modulated vibrations the curve of fig. 6, by modulation on the carrier wave f_A, gives the interference curve *(1)*, the curve of fig. 8 by modulation on the carrier wave f_B gives the threshold curve *(2)*. The shaded difference between these two curves is the attenuation required at every frequency between A and B'. This attenuation is also plotted *(curve 3)*.

Division of the damping among the different filters

In the beginning it was pointed out that there are four filters along the path between A and B': low-pass filter and bandpass filter at the transmitting end and the same at the receiving end. As soon as the total necessary attenuation is determined the question arises as to how this attenuation must be divided among the four filters.

In order to obtain some insight into this question we first ask whether four filters are actually needed. The fact that at least two are needed is immediately clear when it is kept in mind that not only is a certain attenuation required between A and B' but also a certain transmission between A and A' as well as between B and B'. A filter at A can furnish no contribution to the attenuation in the frequency region of the upper side band of f_A, since this side band is just the one used for the transmission from A to A' (*fig. 10*). In this frequency region therefore the attenuation required according to fig. 9 can only be furnished by a filter at B'. For the same reason, however, a filter at B' can furnish no contribution to the attenuation in the upper side band of f_B, so that a filter is necessary at A for this purpose.

If we now try to get along with two filters it becomes clear in a similar way that these two filters cannot be low-pass filters. With the above-described transference of the attenuation curves lying in the region of audio-frequencies to the frequency region of the modulated vibrations every low-pass filter furnishes two symmetrical branches, and according to fig. 10, since no low-pass filter may have any attenuation up to about 3000 c/sec, no attenuation can be obtained in the largest part of the region between the neighbouring carrier waves f_A and f_B.

At least two band-pass filters are therefore needed. The fact that actually two low-pass filters are made to cooperate in the total attenuation is due mainly to economic considerations. The same fact which makes it impossible to get along with low-pass filters only, namely the occurrence of two symmetrical branches of the attenuation curve in the frequency region of the modulated vibrations, also makes it possible to gain double advantage from each attenuation contribution of the low-pass filters,

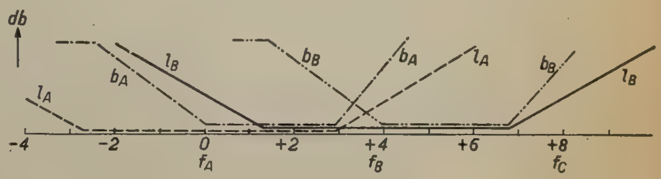

Fig. 10. Diagrammatic representation of the contributions which the low-pass filters (l_A and l_B) and the band-pass filters (b_A and b_B) can make to the total attenuation on the traject between A and B'.

to the right and to the left of the corresponding carrier wave. Moreover, in the case of low-pass filters it is much easier than in the case of band-pass filters to make the attenuation curves sharp, *i.e.* with only slight rounding off in the neighbourhood of the limits of the regions transmitted, a very desirable property for securing the uniform transmission of all the frequencies necessary for the conversation. These facts make it desirable from the economical point of view to have as much as possible of the damping provided by low-pass filters, and to use the band-pass filters mainly for the frequency region mentioned lying between the carrier waves, where the low-pass filters cannot offer any help.

There are, however, other considerations, only secondarily connected with cross talk, which limit the applicability of this conclusion. In the first place in the desired transmission from A to A' (or from B to B') the whole of the lower side band which is not used must be adequately suppressed. If parts of this side band still come through with appreciable intensity then they will amplify the demodulated desired side bands for some frequencies and for others weaken it, according to the phase rotation which the vibrations with the freqencies in question experience in the filters. The fidelity would suffer thereby. For the suppression of the undesired side bands, in which as a matter of fact the low-pass filters cannot help, a damping of at least 35 db is necessary at every frequency in this region, which damping can be distributed equally over the two collaborating band-pass filters at the transmitting and receiving ends.

Another consideration which makes for entrusting a large share of the total attenuation to the band-pass filters is the fact that the energy of the incoming signal at the receiving end is divided among all the channels in ratios which are determined by the attenuation of the different band filters. It is of course desirable to allow as little as possible of the available signal energy to be taken from the desired channel by the undesired channels, and this is ensured by giving the band-pass filters a large attenuation in the attenuated bands.

Practical construction of the filters

After an idea has been formed on the basis of these and other considerations about the way in which the required attenuation must be divided among the filters, it must be ascertained how each filter must be built up in order to obtain the attenuation curve in question. No other practical method for doing this can be suggested than that of trial based upon a knowledge of the properties of a number of simple types of filter sections and the changes which these properties undergo upon variation of the elements of the sections (self-inductances, capacities, resistances). In this process of trial the projected division of the attenuation among the filters will be somewhat modified by several practical considerations: the smallest possible number of filter elements is desired, the number of sections in each filter must of course be the whole number ⁵), and it is an advantage in manufacture to reduce to a minimum the number of types of filters in the installation.

In this way the filter connections given in *figs. 11* and *12* were derived for the above-mentioned 17-channel system of Philips. The low-pass filters are identical for all channels but differ at the transmitting and receiving ends, which is to be understood considering the asymmetrical shape of the required attenuation curve according to fig. 9. The band-pass filters at the transmitting and receiving ends are made similar in the main, and as far as possible they are always built up of the same types of sections, but of course with different values of the capacities and self-inductances for each channel (each carrier-wave frequency).

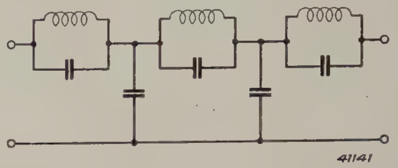

Fig. 11. Structure of the low-pass filters in the 17-channel system. At the transmitting and receiving ends filters of the same configuration are used but with slightly differing values of the elements and thus also with different attenuation characteristics.

We shall here give a few particulars of the construction of the filters. The band-pass filters for the various channels are connected in parallel at the transmitting end as well as at the receiving end. The end branches of these filters must therefore be so composed that the various filters connected in parallel do not affect each other unfavourably. For this purpose the correction element I indicated in fig. 12. is added. Furthermore, the bandwidth $f_{max} - f_{min}$ is the same for all band-pass filters; the *relative* band width

$$(f_{max}-f_{min})/\sqrt{f_{max}\cdot f_{min}}$$

is therefore smallest for the channels with the highest carrier-wave frequencies. As a result the rounding off of the attenuation curves near the limiting frequencies is in general the most pronounced for these channels, and thus the transmission in the pass-band is less uniform. In order to obtain a uniform transmission of all speech frequencies for the higher channels also, a correction element II is now connected in parallel at the input terminals of the filters at the transmitting end of these channels. This element causes a certain extra attenuation in the middle of the pass-band and gives practically no attenuation at the edges. Due to this device the total attenuation of the channel in question is of course several db greater, but this can easily be compensated in the corresponding channel repeater.

The attenuation curves realized with the four filters for one of the middle channels are shown in *figs. 13a* and *b*, while in *fig. 14a* the total attenuation curve between A and B obtained from them by addition is drawn, together with the curve derived above for the minimum required attenuation (curve *3* of fig. 9). In the same way in fig. 14*b* the total attenuation ob-

---

⁵) Half cells are actually also possible, but as a rule their use is not very economical.

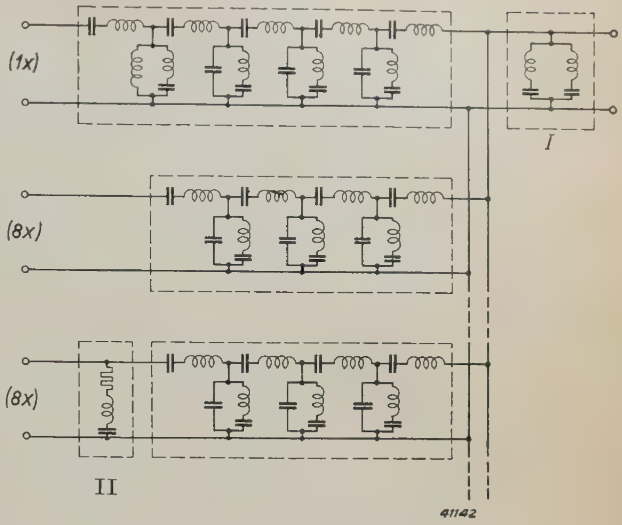

Fig. 12. Structure of the 17 band-pass filters at one end connected in parallel. The first band-pass filter (for the channel with 4 kc-sec as carrier-wave frequency) has a different structure, the other 16 (with 8 to 68 kc/sec as carrier-wave frequencies) are composed of the same types of filter sections. The topmost 8 transmitting filters also contain a correction element *II*; this element is unnecessary in the case of the receiving filters. In parallel with the common end of the band-pass filters a correction element *I* is introduced for the correct termination without mutual effects of the filters.

tained between C and B' is drawn. The fact that this is not exactly the same as that between A and B' follows simply from the fact that the low-pass filters are not identical at the transmitting and receiving ends. Upon transference of their attenuation curves to the frequency region of the modulated vibrations, in the first case (A to B') the contribution of the transmission low pass filter to the total attenuation lies at the lower limit of the receiving channel, that of the receiving low pass filter at the upper limit. In the second case (B' to C') it is just the reverse. Moreover, the curves for the required minimum attenuation, as already stated, are different for the two cases, *i.e.* they are symmetrically located with respect to f_B.

In both cases, *i.e.* in fig. 14*a* as well as in *b*, it is immediately evident that the attenuation obtained is considerably greater in practically the whole frequency region than the required minimum attenuation. There is only one small frequency region where the surplus is small. The obvious question is whether this does not mean a waste. The answer must be that on the one hand it is impossible with simpler filters to satisfy the requirement that the attenuation obtained should never fall below the desired attenuation curve at any frequency, while on the other hand an advantage is obtained with the extra attenuation. It may be recalled that in fixing the attenuation requirements we began with the intensity level which was exceeded in speech once every 3 seconds in each half octave. It is now evident that with the attenuation curve obtained this actually leads to the result that, as was considered permissible, a total of one interference is heard no more than once in three seconds. Only in a frequency region about one half an octave wide do the desired and the actual attenuation curves approach each other so closely that at this point

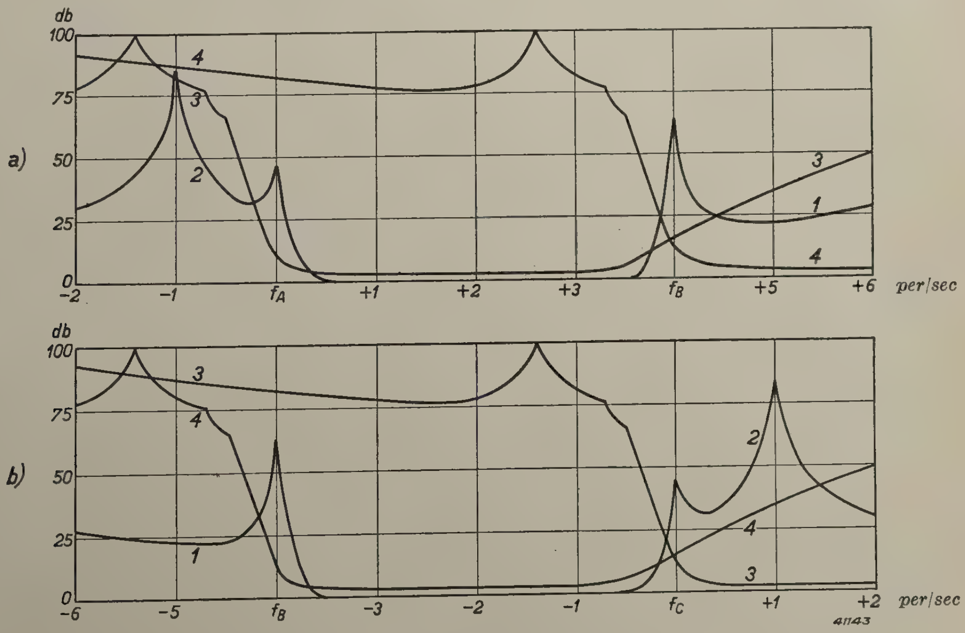

Fig. 13. The attenuation of the filters between two neighbouring channels obtained with the finished installation plotted in the frequency region of the modulated vibrations. *1* and *2* contributions of the low-pass filters, *3* and *4* of the band-pass filters at transmitting and receiving ends, respectively.
a) Attenuation on the traject from A to B ($f_{B'} < f_A$).
b) Attenuation on the traject from C to B ($f_{B'} > f_C$).

the permissible interference reaches the unintended subscriber almost in full. Where this half octave would lie in the whole frequency region could not be foretold in advance, but we now see that indeed only a single half octave, instead of every half octave, of the total frequency region had to be taken into account.

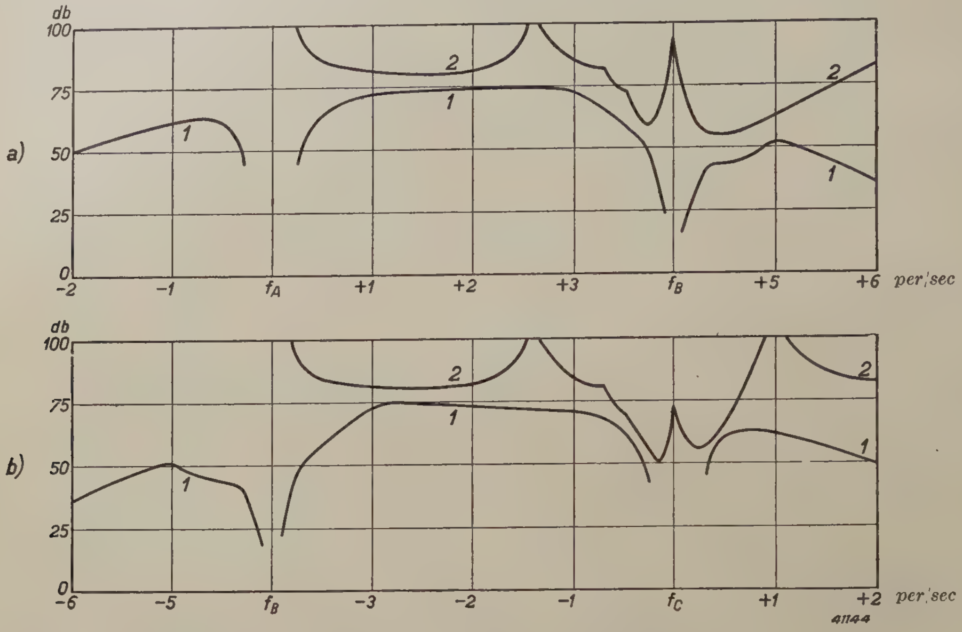

Fig. 14. Comparison of the required attenuation characteristic (*1*) and that actually obtained (*2*) between two neighbouring channels: *a*) from *A* to *B*', *b*) from *C* to *B*'.

Moreover, we based our derivation on the cross talk between neighbouring channels, while we stated above also that more distant channels, due to all kinds of by-products occurring upon modulation [6]), may cause cross talk. For the suppression of just these interference contributions the extra attenuation of the filters is very convenient. The fact that it is actually able to suppress this interference adequately was found to be true in measurements of cross talk with the psophometer in the case of the finished installation.

These measurements were carried out for different speakers in different languages. The level of interference found agreed extraordinarily well with what was assumed as permissible level of interference in our derivation of the damping requirements, while the transmission in each channel was found to be sufficiently uniform for all frequencies between 300 and 3400 c/sec. This shows not only that the method of derivation indicated is correct in spite of several not absolutely sure assumptions which were made, but also that in this way the installation has been successfully made to comply with the requirements: it is good enough, but not unnecessarily good, *i.e.* not more complicated and expensive than necessary.

---

[6]) See the second of the articles cited in note [1]).

THE LOCALIZATION OF CABLE FLAWS

by W. HONDIUS BOLDINGH. 621.317.733:621.317.333.4:621 315.2

A description is given of a measuring bridge for 50 kV protected against high voltage, which, in combination with a high voltage generator for DC voltage, is used for the localization of cable flaws. The conditions are examined which must be satisfied by the connections and especially by the galvanometer in order to combine great strength with great accuracy.

Introduction

The way in which power cables can be tested with high DC voltage has already been described in this periodical [1]). In testing a cable by this method when an abnormally low insulation resistance is found the problem is to find the position of the defect in the insulation as accurately as possible. The usual method of doing this is to carbonize the insulation at the point of the flaw by means of the current provided by the DC voltage generator, so that the defective spot can be localized with a low-voltage measuring bridge.

The latter is usually done by the loop method of Murray: the defective conductor is connected with an intact conductor at one end of the cable, a measuring bridge is connected with the other end and the source of voltage connected between measuring bridge and earth. In this way the ratio can be determined of the resistance x of the part of the defective conductor on one side of the flaw to that of the other part increased by the resistance r of the intact conductor (see *fig. 1*). This method has the advantage that the resistance of the flaw itself does not occur in the localization calculations.

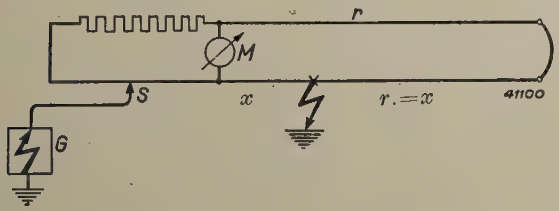

Fig. 1. Localization of a cable flaw by the loop method of Murray. The resistance of an undamaged cable conductor is r, while the resistances of the two sections of cable at either side of the flaw are x and r-x. G is the high-voltage generator and M the galvanometer. In the left-hand part of the bridge, by means of a slide wire, the ratio of the resistances of the two branches is made equal to that in the right-hand part. On the slide wire S the distance of the flaw is read off as a percentage of the length of the cable.

It is clear that the accuracy with which the position of the flaw can be determined depends upon the current which can be sent through the insulation flaw. There will be a certain minimum current at which satisfactory measurement is just possible. It therefore depends upon the resistance of the flaw how much *voltage* is needed for the measurement.

Now it is often found to be very difficult,or to require much time, to burn the insulation through to such a degree that reliable measurement with a low-voltage measuring bridge is possible. The case may even occur in which indeed an abnormally low insulation resistance is measured, but upon long continued testing at the highest permissible or available voltage the current remains low. A sensitive measuring bridge is then needed which must be able to remain under high voltage during the measurement.

For the localization of flaws under these circumstances measuring bridges have been improvised and even offered for sale in a more technical form, which, in combination with a cable testing apparatus, make possible measurements under high voltage. These measuring bridges consist chiefly of an adjustable resistance (decade resistance or slide wire) and a galvanometer, which are insulated together for the full voltage and placed for instance on a tripod of insulation material, and which can be adjusted and read while under tension.

The remarks in our previous article [1]) about the danger of high voltage in the case of cable testing generators is even truer for the measuring bridges: in this case as a rule there is not the least protection against high voltage for the operator. It was therefore important, in addition to the cable testing generator with protection against high voltage, to design a measuring bridge offering the same degree of safety.

We shall now describe such an apparatus which was constructed for a voltage of 50 kV.

Galvanometer

The centre of the cable measuring bridge is of course the galvanometer. In the first place the accuracy of the localization depends upon the sensitivity of this instrument, and in the second place the form of the apparatus is determined by the manner of reading the galvanometer under high tension.

The advantages of a reflecting galvanometer are immediately obvious: it is very sensitive because the moving indicator is a beam of light and a beam of light is an ideally insulated, long and weightless "pointer" between the galvanometer under high tension and the earthed reading scale. Disadvantages of the reflecting galvanometer are its fairly large dimensions and its low resistance to mechanical and electrical shocks. Although in recent years so-called light-spot galvanometers which are transportable have appeared on the market, which constitute a considerable improvement in this line, they cannot immediately be used for the localization of cable flaws.

---

[1]) Philips techn. Rev. 7, 59, 1942.

A galvanometer has now been successfully constructed which, because of its small dimensions, great sensitivity and high mechanical and electrical resistance, is particularly suitable for the object in view. Advantage was taken of the use of a modern magnet steel of high magnetic power [2]), with which a strong field in a relatively wide air gap can be obtained with small weight and dimensions of the permanent magnet. This makes it possible to give the galvanometer coil a large number of windings with a given resistance. In this way, in spite of the use of a strong suspending wire, the power necessary for a deflection of one scale division could be reduced to several tenths of a picowatt (10^{-12} W).

Fig. 2 is a photograph of the galvanometer. The rotating coil together with the mirror is suspended on a stretched wire; the wire has the cross section of a ribbon. To a large extent it is the properties of this ribbon which determine the quality of the galvanometer: the ribbon must submit easily to torsion in order to produce a high sensitivity, but at the same time a relatively thick ribbon is desirable for the sake of mechanical strength and electrical resistance to current impulses. As for the latter, the ribbon form is especially favourable, and we shall discuss this point later.

The accuracy of the localization

Considering the fact that the opening of a cable sleeve or the digging up of a section of cable costs considerable time and money, and that a cable must only be out of use for as short a time as possible, the rapid and accurate localization of a flaw is of the greatest importance. Various sources of error outside the measuring bridge may affect the accuracy of measurement. Thus, for example, the tolerance of the copper cross section of the cable sets a limit to the accuracy with which the position can be deduced from a measurement of the resistance of a cable conductor. Thermo-forces in the measuring circuit, stray currents in the ground or corona losses in the switching apparatus at the end of the cable may disturb the measurements. Finally the normal insulation resistance of the cable may cause an error in the localization.

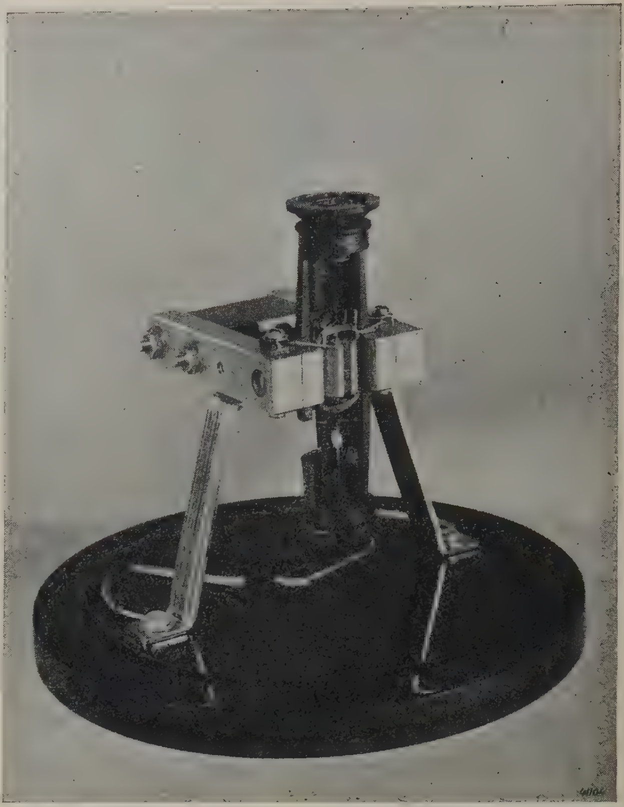

Fig. 2. View of the galvanometer, whose total height is 8 cm.

In this article we shall leave such sources of error out of consideration and confine ourselves to the theoretical accuracy of the localization. Assume that the measuring bridge can be adjusted continuously (with a slide wire) and that the scale can be read with an accuracy of one millimeter. The question is then what error, expressed in meters of cable, will be made in localization if the galvanometer is not set exactly at zero but has a deflection of 1 mm. If we express this length λ, which we shall call the inaccuracy of localization, in quantities pertaining to the measuring circuit, we can study how the influence of this error in reading can be limited to a minimum, and thus how the localization can be made as accurate as possible.

Let us call

the direct current through the insulation flaw i mA,

the resistance of the slide wire R_s ohm,

the resistance of the galvanometer R_g ohm,

the voltage constant of the galvanometer u_g μV/mm,

the resistance per meter cable length r_1 ohmm,

the cable resistance (one lead and return) R_k ohm.

---

[2]) Philips techn. Rev. 5, 29, 1940 and 6, 8, 1941.

By application of Kirchhoff's laws we then find that

$$\lambda = \frac{0.001\, u_g}{i r_1}\left(1 + \frac{R_k}{R_g} + \frac{R_k}{R_s}\right) \;.\;. \quad (1)$$

From this it appears in the first place that λ is independent of the position x of the flaw. In the second place it is clear, as it was also without the formula, that the inaccuracy of localization is inversely proportional to the current i. In the third place it follows from formula (1) that R_s must be large compared with R_k. This last condition can easily be satisfied, as will appear later.

When the galvanometer resistance R_g is also large compared with the cable resistance R_k, which is usually the case with the instruments used for this purpose, the formula for the inaccuracy of localization *for 1 mA*, λi in the case of cables with a copper cross section of Q mm² becomes:

$$\lambda i = \frac{0.001\, u_g}{r_1} = 0.057\, Q \cdot u_g \;.\;.\;.\;.\;. \quad (2)$$

It is found that in this case ($R_g \gg R_k$) the product λi depends exclusively upon the copper cross section Q, so that the accuracy of the localization is independent of the length of cable.

The conclusion must not, however, be drawn that the greatest accuracy is obtained with $R_g \gg R_k$: I_g and u_g are not independent variables and must therefore be considered in their mutual relation.

For this purpose we disregard in formula (1) the quantity $R_k/R_s \ll 1$ and write the formula as follows:

$$\lambda = \frac{0.001}{i r_1}\,(u_g + i_g R_k), \;.\;.\;.\;.\;. \quad (3)$$

where $i_g = R_g/u_g$ is the current constant of the galvanometer in μA per scale division. Since $u_g \cdot i_g = W_g$, the so-called power constant, is a more or less constant quantity of the galvanometer independent of the resistance R_g, λ is a minimum for

$$u_g = i_g R_k, \quad \text{thus} \quad R_g = R_k.$$

The most favourable conditions for the measuring circuit are therefore when

galvanometer resistance =
cable resistance $\ll$ comparison resistance.

When in this way the galvanometer has its optimum adaptation to the cable resistance ($R_g = R_k$), and taking into account that $R_g = R_k = 2000\, L r_1$, where L is the cable length in kilometers, one finds that

$$\lambda_{\min} \cdot i = 0.68 \sqrt{W_g Q L}.$$

The minimum inaccuracy of localization is thus proportional to the square root of the volume of copper QL.

It must, however, be taken into account that the cable resistance varies between wide limits, so that R_g is not always equal to R_k. In practice

Q will vary from 25 to 150 mm², and
L ,, ,, ,, 0.2 to 10 km.

Of course the cables, as a whole, are always longer than 0.2 km and sometimes longer than 10 km, but for the localization of a flaw the shortest possible length will always be chosen for measurement. When in addition we take into account the fact that thin cables as a rule are not very long, we can calculate that the resistance of the length measured, out and back, will vary between about 0.05 and 5 ohms.

The most unfavourable combination is that with the largest copper volume: $L = 10$ km, $Q = 150$ mm². In this case $R_k = 2.3$ ohms. If we choose approximately this value of the resistance for the galvanometer we find for the most unfavourable practical case:

$$\lambda i = 0.68 \sqrt{10 \cdot 150\; W_g} = 26 \sqrt{W_g}.$$

A galvanometer with $W_g = 0.5$ pW/scale division², $R_g = 2$ ohms, *i.e.* $i_g = 0.5\ \mu$A and $u_g = 1.0\ \mu$V per scale division, with 1 mA measuring current will give a theoretical inaccuracy of 18 meters for a cable of 150 mm² and 10 km length. To calculate this for other cases we use formula (3), which is reduced to:

$$\lambda i = 0.057\, Q u_g + 2\, L i_g \;.\;.\;.\;.\;.\;.\;.\;.\;. \quad (4)$$

For a shorter length or a smaller cross section the inaccuracy of localization for 1 mA may fall to 9 m, for a shorter length and in addition a thinner cable, for instance 200 m, 25 mm², it may even fall to 2.2 m (see *fig. 3*).

If the galvanometer resistance were 200 ohms instead of 2 ohms with the same power constant $W_g = 0.5$ pW, u_g would equal 10 μV and the inaccuracy of localization would be 5 to 10 times as large.

In *fig. 4* with different system resistances from 2 to 200 ohms λi is given as a function of the cable length for a meter of 0.5 pW and a cable of 150 mm². From this figure the advantage can clearly be seen of the optimum adaptation of the galvanometer resistance.

With a galvanometer of the type described above, with a well adapted resistance, therefore, with no more than 1 mA through the cable flaw a very satisfactory theoretical accuracy of localization can be obtained.

Mechanical and electrical resistance

Notwithstanding its high sensitivity the galvanometer is very resistant to the mechanical and electrical shocks which may occur in cable measurement. The complete measuring bridge in all positions with short-circuited but unlocked galvanometer can be carried on a car with massive rubber tyres over a very uneven pavement without the zero position undergoing appreciable change. An absolutely horizontal position during the measurement is not required.

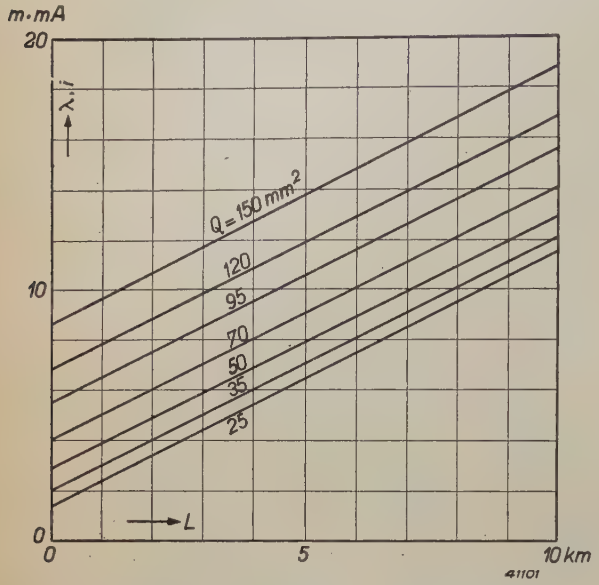

Fig. 3. Theoretical inaccuracy of localization λ in metres times the current i in mA as a function of the cable length L in km with different areas of copper cross section Q in mm². The resistance R_g of the galvanometer is 2 ohms, the current constant is i_g = 0.5 μA per scale division and the voltage constant u_g = 1.0 μV per scale division.

The electrical dangers to which the galvanometer of a cable measuring bridge is exposed are many. Under various circumstances the galvanometer may receive current impulses which are many thousand times as great as those which cause a normal large deflection. It should be required of a measuring bridge for the localization of cable flaws that it be proof against all the catastrophes which may occur during a measurement and which cannot be avoided by reasonably good operation. On the basis of the connections in *fig. 5* we shall now study the different incidents which may occur.

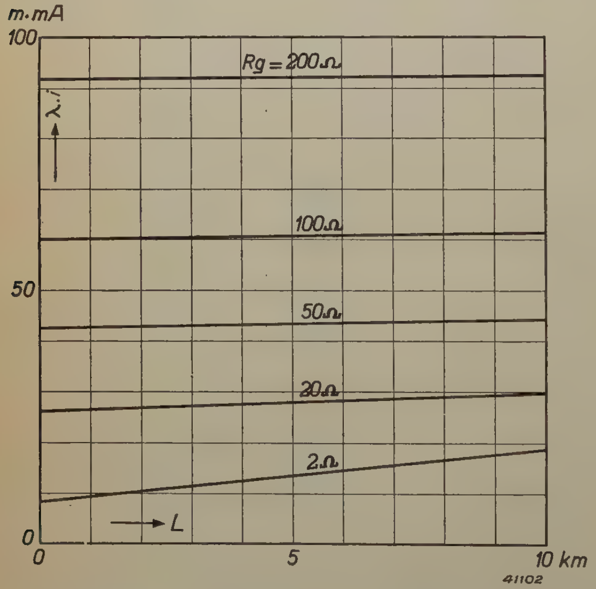

Fig. 4. Theoretical inaccuracy of localization in metres at 1 mA (λi) for a cable of 150 mm² cross section as a function of the cable length L in km and for a galvanometer with a power constant W_g = 0.5 pW per scale division². The resistance R_g of the galvanometer is taken at 2, 20, 50, 100 and 200 ohms, respectively.

The most serious case is that in which during a measurement on a long cable at full voltage the flaw suddenly breaks down. In the first place a voltage surge may thereby occur on the terminals G_1 and G_2 of the two conductors between which the galvanometer is connected, and in the second place the DC voltage generator will suddenly begin to give a high charging current, which *via* S flows through the measuring bridge and, before it is switched off by an automat, may be several hundred times as large as the original measuring current. If the bridge is already in equilibrium this will not be so serious, but the breakdown may occur before the bridge is balanced.

Another case which must be considered is a discharge of the cable due to earthing of the high-tension pole of the generator (point S), either expressly, in order to earth the cable, or unexpectedly upon the breakdown of a safety spark gap. As a rule this takes place over an earthing resistance, in the previously described cable testing apparatus over a built-in fixed resistance with magnetic switch or spark gap. Upon such a discharge the discharging current, which may amount for a short time to several amperes, flows through the measuring bridge. Considering the fact that the total comparison resistance amounts to 4000 ohms, a high voltage would occur between S_1, S_2, and S. This is limited by two rare-gas cartridges across S-S_1 and S-S_2. Further protection is, however, impossible without unfavourable effect on the accuracy of measurement; the galvanometer must therefore be able to tolerate the remaining difference between the voltages on the two branches of the comparison resistance in all points of balance of the bridge, and even when the bridge is completely unbalanced and preferably then also at maximum sensitivity.

It has been found that even with a cable capacity of 12 μF charged to 50 kV, *i.e.* an energy of 15 kW sec, the above-mentioned requirements can be satisfied even with a discharge over only a few thousand ohms. Only in the case of a complete breakdown of the cable in the neighbourhood of the measuring bridge is the galvanometer inevitably ruined when it is connected in its most sensitive state. The chance of such a combination of unfavourable circumstances, however, is very slight.

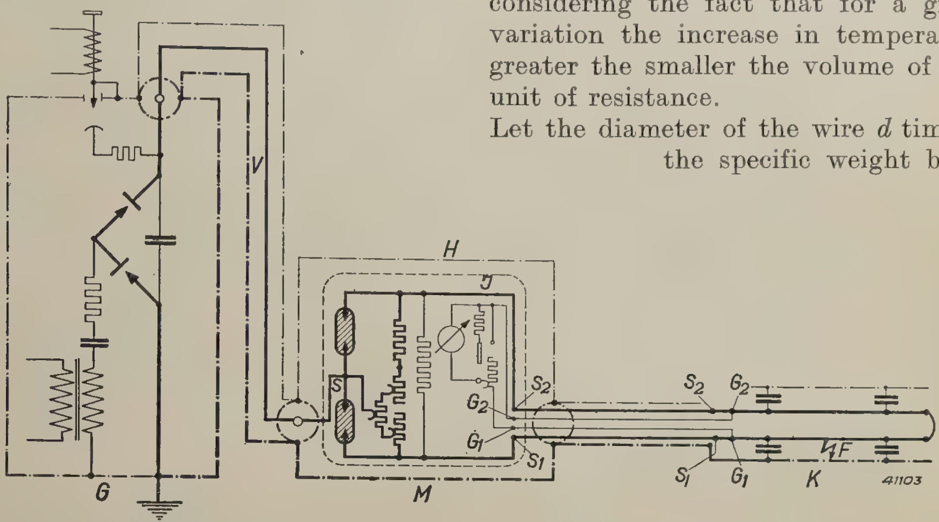

Fig. 5. Diagram of the connections of the installation for the localization of cable flaws, consisting of the previously described [1]) cable testing generator *G* which is joined by a short connection cable *V* to the cable measuring bridge *M* described in this article. Surrounding the whole a covering *H* proof against high voltage is indicated, part of it with a thick line to indicate the high-voltage circuit. All parts within the broken line *I* are insulated for 50 kV toward earth. *K* is the cable in which a flaw *F* must be localized. The high-voltage terminal of the generator is connected with point *S*. The voltages between point *S* and the points S_1 and S_2 of the cable conductors to be measured are limited by rare-gas cartridges; the galvanometer is connected between the terminals G_1 and G_2 of the measuring conductors. The connection between the measuring bridge *M* and the cable to be measured *K* is by means of a long connection cable. This cable has 4 conductors in order that the resistance of the connection lines and the transition resistance of the terminals may have no effect on the accuracy of the localization.

In other cases, however, the amount of energy which flows through the galvanometer circuit may still be of such a nature that the meter must have an unusually high resistance against the electrical shock which a current impulse causes in the system. A mechanical impulse then occurs and a heating of coil and suspension wire. In addition to the fact that the electrical damping is very strong due to the strong magnetic field and the low ohmic resistance in the circuit, the rotating coil can be mechanically damped after a small deflection, since it is here a question of a zero instrument where large deflections are unnecessary and unwanted. The mechanical impulse can be taken up without danger.

The thermal resistance of a rotating coil of about 2 ohms is very large. When 1 A flows continuously through the coil only 2 W are taken up, which the coil can easily tolerate. A current impulse may still attain a much higher value without overheating the coil. It is clear that in the last case the suspension wire is the weakest point. This can, however, withstand much more than would be expected in such a sensitive instrument. Thus a ribbon of the galvanometer used here can conduct 1 A continuously without reaching the melting temperature, since the heat developed can be adequately dissipated. In the case of a current impulse which lasts for less than for instance 0.1 sec, however, cooling plays no part. In that case it is a question of the *heat capacity per ohm*, considering the fact that for a given current variation the increase in temperature will be greater the smaller the volume of the wire per unit of resistance.

Let the diameter of the wire *d* times *b* equal *q*,
the specific weight be *s*,
the heat capacity *c*,
the specific resistance r_1.

Then, if we also take into account the fact that $W_g \sim d^3 b$, the heat capacity per ohm becomes proportional to

$$\frac{W_g{}^2 \cdot s \cdot c}{d^4 \cdot r_1}.$$

In contrast to the case with a discharging resistance, the specific resistance must here be low; silver or copper-silver is therefore chosen. It is found further that a flat suspension ribbon is more important here than in galvanometers with continuous loading; *with a given sensitivity the thermal resistance is inversely proportional to the fourth power of the thickness of the ribbon.*

The application of these conclusions has made it possible to satisfy the requirements of strength without sacrificing part of the sensitivity.

Time to reach a steady deflection

It is mainly the time necessary to obtain a steady deflection which sets a practical limit to the sensitivity of a galvanometer. Due to the light weight the characteristic vibration time of the system is indeed always relatively short, but due to the low internal resistance (about 2 ohms) and an external resistance which sometimes almost amounts to a short circuit, the adjustment to a steady deflection becomes of the dead beat type.

Although the above-mentioned quantities for the galvanometer (0.5 μA and 1.0 μV) are not the most extreme values attainable, this construction is chosen in order to obtain a dead beat deflection of not more than a few seconds. The sensitivity is still so great that increasing it would bring no appreciable improvement due to the unavoidable external sources of disturbance.

With a switch which can short circuit the galvanometer the sensitivity can also be made 10, 100, 1000 and 10 000 times as small. Upon decreasing the sensitivity the galvanometer circuit is made almost aperiodic with a time for reaching steady deflection of less than 1 sec.

Comparison resistance

For a continuously regulable zero adjustment of the galvanometer in bridge connections a stretched resistance wire with sliding contact is theoretically the best method. When, however, the value of the resistance must be large compared with galvanometer and cable resistance, for instance 100 ohms, the length of the wire must be very great or the wire so thin that its cross section cannot be considered constant, so that a special calibration is necessary. Still worse is the fact that the wire will be worn more at certain spots than at others, so that the calibration becomes valueless and a precise measurement complicated.

It is much better to choose a resistance in steps of the type of a decade resistance (see fig. 5). Because of the fact that 10 times 10 positions are too few for an accurate balancing, and that it is undesirable to have more than two adjusting knobs, 20 times 20 positions were chosen. Moreover, an equally large fixed resistance is connected in series with the variable resistance, so that the balancing can be done with only one half, corresponding to the resistance of the defective cable conductor; the fixed resistance corresponds to the undefective return conductor.

In this way one stage for fine regulation corresponds to 2.5 per thousand of the cable length, *i.e.* to 2.5 meters per km. Suppose that the measuring length of a cable is 10 km and the theoretical inaccuracy of localization amounts to 2.5 metres. Then one stage for fine regulation will correspond to 25 metres of cable, thus with a galvanometer deflection of 10 scale divisions. By interpolation the position of the flaw can be found to within 2.5 metres. With a cable length of 1 km this would even be possible without interpolation.

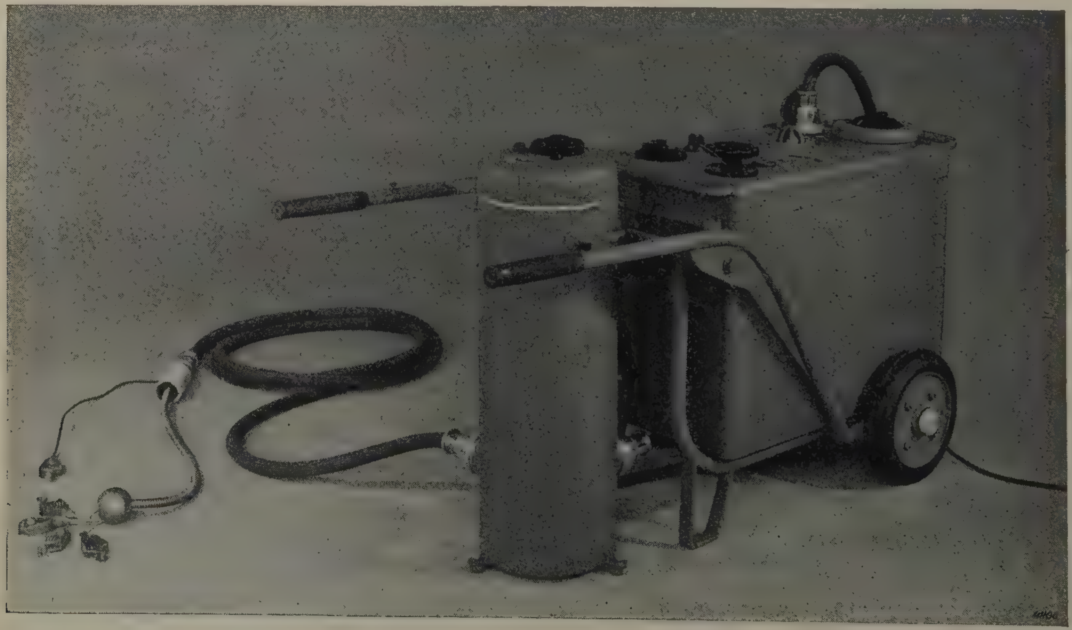

Fig. 6. The complete apparatus for the localization of cable flaws, consisting of the cable testing generator for 20 kV and the cable measuring bridge.

Construction

Fig. 6 shows the combination of the measuring bridge with the generator for 20 kV. *Fig. 7* shows the high voltage part of the measuring bridge and *fig. 8* the interior of the same.

It may be seen that the whole measuring bridge including safety elements and sensitivity adjustment of the galvanometer is housed in a well rounded can which is insulated from and fastened to a cover plate upon which the light source and scale of the galvanometer are mountted. The comparison resistance is varied from above by means of two concentric insulated shafts. Beside them are two other insulated shafts, one for the sensitivity regulation and one for zero point correction.

The whole galvanometer circuit (with the exception of the connection terminals) is enclosed in the above-mentioned can, which thus shields the circuit as a Faraday cage and which is itself connected with point S of the high-voltage circuit (see fig. 5). By this means any corona losses and leakage currents are kept outside the measuring circuit, so that they can have no unfavourable effect on the accuracy of the localization.

The high voltage part is placed in a metal cylinder, see fig. 7, into the lower part of which two connections for high-voltage-proof connection cables are screwed for the connection with the high-voltage generator and the cable to be measured, respectively. By this means the whole exterior is connected *via* the braided metal cable covering with the mass of the generator to be earthed, so that there is nowhere any part under tension which can be touched. The insulation between the high-voltage part and the earthed housing with operation knobs is calculated for 50 kV.

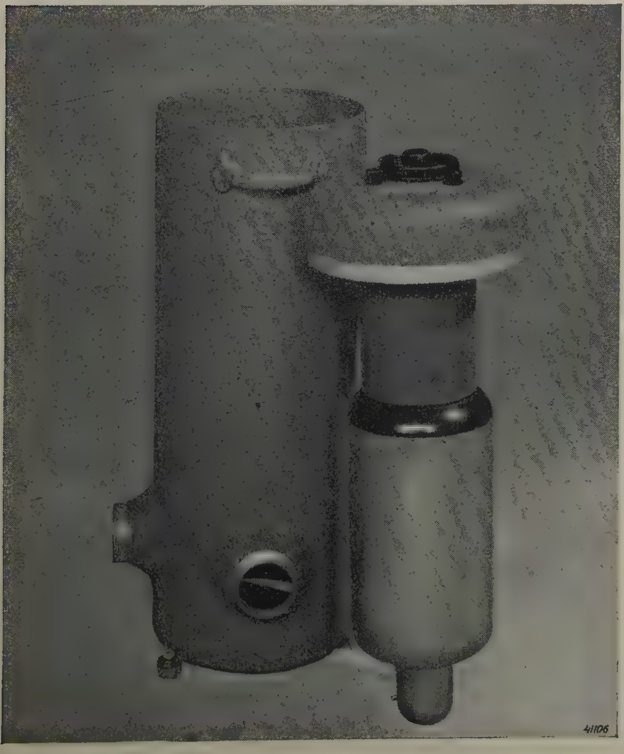

Fig. 7. High voltage part of the cable measuring bridge.

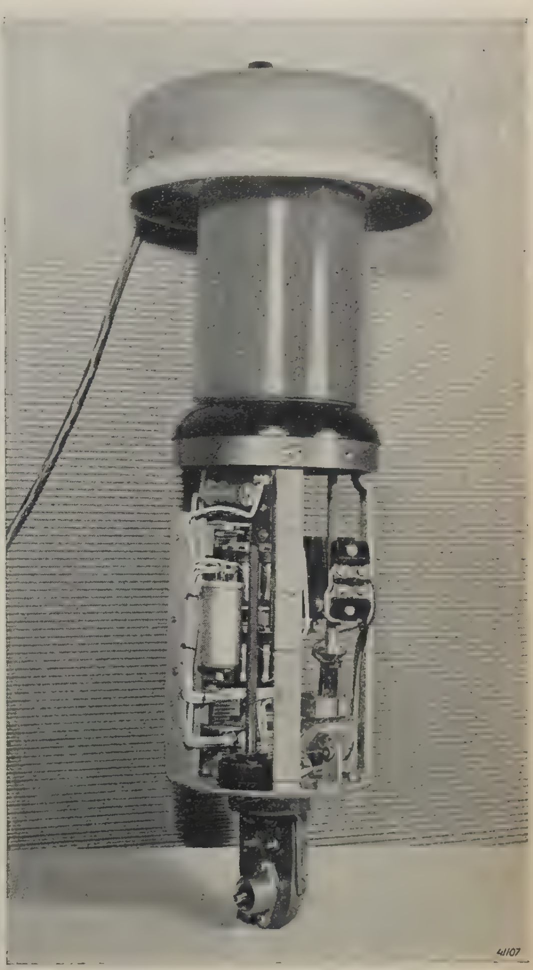

Fig. 8. View of the interior of the high voltage part.

Measuring voltage

Although cables which must be tested with voltages higher than 50 kV are no exception, and cable testing apparatus are therefore also necessary for higher voltages than 50 kV, in general an attempt will be made to limit the voltage for the localization of flaws to 50 kV, since at higher voltages the corona losses at the point of connection with the cable to be measured may be disturbing.

In this respect a sensitive measuring bridge which makes it possible to carry out the measurement with a lower current and therefore a lower voltage, is of particular value: with a measuring bridge which is five times as sensitive as another the same theoretical accuracy of localization can be attained with five times as low a voltage. The limit to this decrease of the voltage is set only by certain sources of error which are *independent* of the measuring voltage. In general, with the measuring bridge here described the best results will be obtained with measuring currents between 1 and 10 mA.

THE TEXTURE OF CROSS-ROLLED MOLYBDENUM

by J. F. H. CUSTERS.

620.18

When cold-rolling molybdenum which crystallizes in a body-centred cubic lattice and especially during cross-rolling employed practically, a typical texture may appear which differs entirely from the previously discussed rolling texture of certain face-centred cubic crystalline metals. In the case of molybdenum strip for technical applications measures are taken to prevent this texture, while in an investigation of the elastic behaviour of molybdenum the texture of the cross-rolled material could be used to advantage.

Various metals when rolled in the cold state acquire a texture, *i.e.* the crystal grains of the polycrystalline metal, which originally are arranged at random as far as the directions of their crystallographic axes are concerned, due to the rolling take up more or less sharply distinguished preferential positions. In a previous article attention was called to the rolling texture of nickel-iron alloys and other metals which crystallise in a face-centred cubic lattice (aluminium, copper, etc.). Quite a different rolling texture is found in the case of certain metals which crystallize in the body-centred cubic lattice (see *fig. 1*), such as molybdenum, tungsten, α-iron. In this article we shall study in particular the texture of rolled molybdenum which is used for instance for anodes of transmitting valves and the like, and we shall consider several questions connected with their texture.

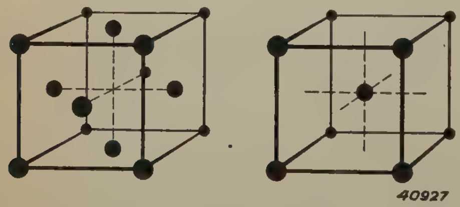

Fig. 1. Positions of the atoms in a face-centred (left) and a body-centred (right) cubic lattice.

The occurrence of rolling textures in general must be pictured in the following way. Due to the mechanical stresses caused by the rolling, displacements take place in each crystal grain along definite lattice planes (slip planes) and in certain directions (slip directions), the grain being very much hampered in its movements by the neighbouring grains. The result is that each grain undergoes not only a complex deformation and a possible splitting up into smaller grains, but also a rotation about definite axes.

The slip planes and directions referred to are different for a face-centred lattice from those for a body-centred lattice, and this constitutes one of the most important reasons for the differences in the textures which occur upon rolling such metal lattices. While upon the rolling of certain face-centred cubic lattices, as was explained in the article cited ¹), the crystal grains mainly take up a preferred position whose correlation with the direction of rolling is quite complicated, the texture which is formed when cold-rolling molybdenum and other metals crystallizing in a body-centred cubic lattice can be characterized rather simply: most of the grains take up such a position after the rolling that one of their six sets of rhombododecahedron planes ²) is perpendicular to the direction of rolling ³). The position of these grains is not in this way fully determined, since a rotation about the direction of rolling as an axis is still possible, as illustrated in *fig. 2*. Indeed in this respect the grains still actually show various orientations, as may be concluded from the X-ray diffraction diagram *fig. 3* .Upon further investigation, however, it is found that the statistical distribution among these orientations is not entirely uniform, but that the grains show a

---

¹) J. F. H. Custers, Philips Techn. Rev. **7**, 45, 1942.

²) A rhombododecahedron plane is a plane passing through diagonally opposite edges of the cube of the crystal lattice.

See also Philips Techn. Rev. **7**, 15, 1942 (fig. 4).

certain preference for a position in which the set of rhombododecahedron planes which lie in the rolling direction is perpendicular to the surface of the rolled strip This preference now becomes almost exclusive when the rolled strip is further rolled in a direction perpendicular to the direction of the first rolling. The strip is then said to be cross-rolled. Upon consideration of fig. 2 it is immediately clear that the freedom in the orientation of the grains remaining after the first rolling will indeed be lost upon the second rolling. In that case the second set of rhombododecahedron planes mentioned must take up a position perpendicular to the new direction of rolling, whereupon the final position appears [3]). As may be seen in the diagram of *fig. 4*, in each grain a cube plane is now parallel to the surface of the rolled strip, while the two other cube planes are perpendicular to this surface and make an angle of 45° with the direction of rolling.

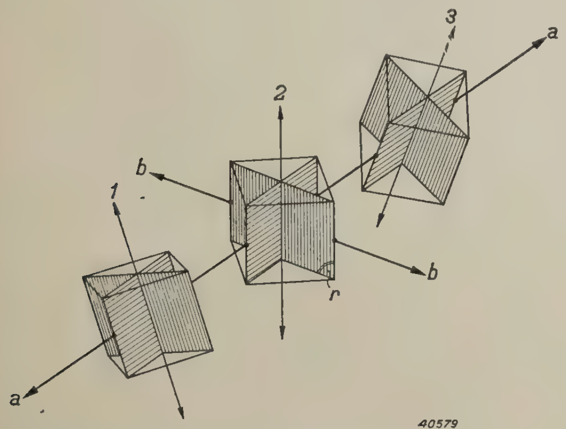

Fig. 2. After rolling, the crystal grains of the polycrystalline molybdenum specimen take up such a position that a rhombododecahedron plane (*r*) is perpendicular to the direction of rolling *a-a*. The rhombododecahedron plane which is parallel to the direction of rolling may still be at different angles with the transverse direction *b-b* of the rolled strip, as is here shown diagrammatically for three grains *1*, *2* and *3*.

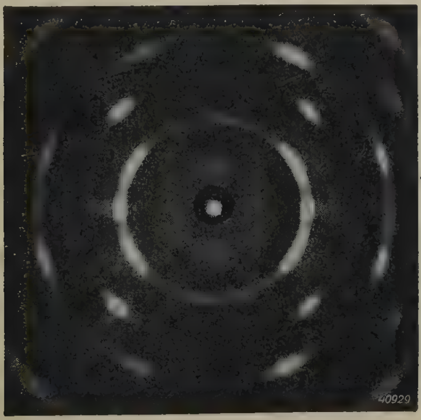

Fig. 3. X-ray diffraction diagram of rolled molybdenum upon normal incidence. The direction of rolling is from the top toward the bottom.

In *fig. 5* an X-ray diffraction photograph is reproduced of cross-rolled molybdenum with normal incidence of the X-rays on the strip. The four-sided symmetry of the texture compared with the only two-sided symmetry of fig. 3 is immediately noticeable. The innermost Debije-Scherrer circle of fig. 5, which here clearly contains four spots, corresponds to reflections at the rhombododecahedron planes. If the ideal position of the grains were fully attained, these four spots would not occur on the photograph, since the X-ray beam would then have a purely glancing incidence along the rhombododecahedron planes, while for reflection a finite angle of incidence (to be derived from Bragg's equation) is required. The fact that the spots, nevertheless, occur thus indicates

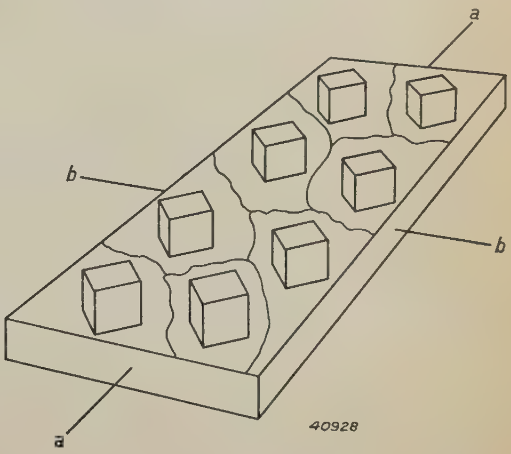

Fig. 4. Position of the crystallographic axes (cube edges) of the separate grains in cross-rolled molybdenum. *a-a* first, *b-b* second rolling direction.

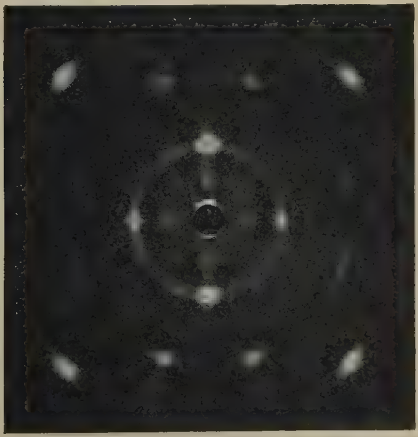

Fig. 5. X-ray diffraction diagram of cross-rolled molybdenum, to be compared with fig. 3.

---

[3]) C. E. Ransley and H. P. Rooksby, Inst. Met. **62**, 205, 1938.

that the grains exhibit a certain scattering about the ideal position. The minimum value of this scattering can be deduced directly from the photograph. Moreover, there are also a number of grains which take no part at all in the preferred orientation described, as may be seen from the fact that in the photograph of fig. 5 the complete Debije-Scherrer circles can still be seen faintly.

If this and the slight scattering mentioned are neglected, cross-rolled molybdenum strip may be considered as a pseudo single crystal: there are indeed crystal boundaries between the different grains, but in all manipulations in which the influence of crystal boundaries may be neglected the strip will behave almost exactly like a single crystal. In particular it will exhibit an anisotropy in some of its mechanical properties. A very striking example of such anisotropy occurs in the case of tungsten, which is closely related to molybdenum. If rolled tungsten strip is annealed somewhat unevenly at a high temperature the stresses occurring in the strip may cause small rectangular bits to spring out of the strip [4]). It is found that the coherence between the crystal grains is least along the cube planes at 45° to the rolling direction. The fact that fissures may appear along such planes upon the occurrence of stresses is also often experienced in severe rolling of tungsten and molybdenum strip in the cold state, whereby cracks may occur in directions at 45° to the direction of rolling.

The texture of rolled, and especially of cross-rolled molybdenum, in the treatment which the strip must undergo for practical application (for anodes for example it must be cold folded and provided with grooves), may therefore lead to difficulties.

Now from an economical point of view cross-rolling is the most suitable method of preparing molybdenum strip. We shall illustrate this by a consideration of the preparation of molybdenum.

Since molybdenum has an unusually high melting point, the metal is not obtained technically from a melt, but as in the case of tungsten the methods of powder metallurgy are applied[5]). The metal is first obtained in the form of a very fine powder by reduction from one of its compounds, the powder is compressed in a matrix to a rod which is then carefully presintered at about 1300° C. Then, when it has somewhat more mechanical strength, it is heated by a very high electric current to the true sintering temperature of about 2000° C. The sintered rod must now be rolled to strip or sheet with a width of for instance 12 cm, while the desired thickness may be for instance 0.2 mm. The largest possible rods are preferred as a starting point. The dimensions of the rod, at least its length, are, however, limited by the low mechanical strength before sintering, and its thickness is limited by the available rolling pressure. These factors lead to the use of rods of the dimensions 12 × 40 × about 200 mm. Such a rod is first hot-rolled transversally, so that, with the length of 20 cm remaining the same, the desired width of 12 cm is obtained. In order to be able to employ not too great a rolling pressure in spite of the work-hardening of the deformed and cooled material the strip of 20 × 12 cm obtained is then further rolled in the direction of length until the desired thickness of 0.2 mm is obtained.

The problem is to prevent the formation during this cross-rolling of a product with the above-described texture, which is unfavourable for further working. This can be done in various ways. The rolled strip already possessing the texture can be subjected to an annealing process above 1300° C. The strip then recrystallizes to give a coarse-grained material entirely without texture, as may be seen from the Laue diagram [6]) of *fig. 6*. In this diagram there is only a limited number of spots, which means that the X-ray beam, which is about 1 mm wide, has encountered only few crystal grains. The spots ares cattered quite at random, which indicates that there is no longer any texture. Such a coarse-grained material, however, has the disadvantage of being very brittle. A different method is therefore usually applied to prevent the occurrence of the rolling texture. After the transverse rolling and during the longitudinal rolling the strip is annealed at a relatively low temperature between successive stages of the rolling. It is found that in this way the rolling texture fails entirely to develop, and at the same time there is the advantage that in the heated state the material can more easily be rolled. This method is used in the practical manufacture of molybdenum strip.

While for practical purposes the object is to avoid the occurrence of the texture during cross-rolling, a case occurred in which advantage could be taken of the texture. It was a question of a comparative study of the elastic constants of several metals carried out in this laboratory [1]). While in measurements on polycrystalline specimens of metal only the average values of the elastic constants (averaged over all the crystallographic directions) are found, for theoretical insight into the elastic behaviour it is desirable

---

[4]) W. G. Burgers and J. J. A. Ploos van Amstel, Physica 3, 1064, 1936.

[5]) See for example J. D. Fast, Philips Techn. Rev. 4, 321, 1939.

[6]) See for example W. G. Burgers, Philips Techn. Rev. 5, 161, 1940.

to determine the constants in the different directions. To do this a single crystal of reasonable dimensions must be available, in this case of molybdenum. Since, however, the preparation of a large molybdenum single crystal is a very laborious task, use was made here of the fact that cross-rolled molybdenum possesses a texture which gives it the character of a pseudo single crystal. The photograph of fig. 5 has already been referred to in this connection, and it was pointed out that a number of crystal grains still occupy positions which deviate entirely from the preferred positions described. It was now found that these grains could also be brought practically into the ideal position by annealing the rolled strip for several minutes at 1200° C (upon annealing at a temperature 100° higher, on the other hand the texture disappears, as we have seen above). In *fig. 7* an X-ray diffraction pattern of the strip thus treated is reproduced. The intermediate segments of the Debije-Scherrer circles which were still visible in fig. 5 have here practically disappeared. The piece of metal has actually become almost a pseudo single crystal. The elasticity measurements could also be carried out satisfactorily with this strip. Incidentally it may be stated that these measurements showed that with molybdenum, in contrast to the cubic crystalline metals of lower melting point, the modulus of elasticity is smaller in the direction of the space diagonal of the cubic lattice than in the direction of the edge. The ratio of the two moduli in the case of molybdenum is 0.81, while with the alkali metals, for example, a value of approximately 5 is found, with gold and silver approximately 2.5.

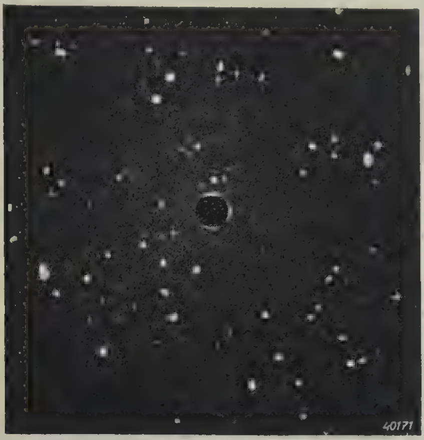

Fig. *6*. Laue photograph of cross-rolled molybdenum which was afterwards annealed at 1300° C. The texture has disappeared entirely. (Laue photographs are made with X-radiation having a continuous spectrum. This is necessary in this case since with monochromatic radiation the few randomly oriented crystal grains present will not in general satisfy Bragg's equation, so that no reflections at all will be obtained. With a continuous spectrum on the other hand there is for every lattice plane in every grain a ray with a wavelength which can be reflected).

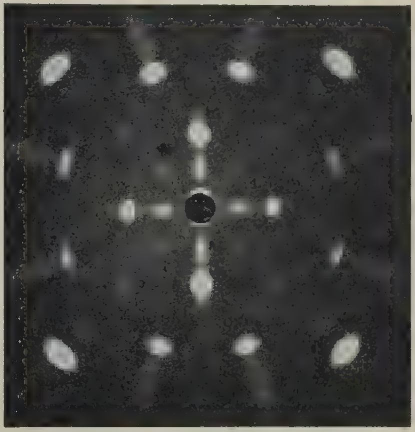

Fig. 7. X-ray diffraction diagram of cross-rolled molybdenum which was afterwards annealed at 1200° C. The texture in this case has become still sharper ; in particular the grains which did not yet occupy the desired orientation and which led to the appearance of the complete Debije-Scherrer circles have now disappeared.

---

[7] M. J. Druyvesteyn, Physica **8**, 439, 1941. For the method of measurement see Philips techn. Rev. **6**, 372, 1941.

A DIODE FOR THE MEASUREMENT OF VOLTAGES

by M. J. O. STRUTT and K. S. KNOL.

621.385.2:621.3.029.6

A diode may be used to measure high-frequency AC voltages. In this article the problems are discussed which occur when this method is applied in the frequency region of decimetre waves. The problems are of the same type as those encountered in other applications of electronic valves in the region of decimetre waves. According to the principles which are applied in the construction of receiving valves for short waves a measuring diode was constructed, which can be used to a wavelength of 30 cm. In conclusion several other details of the measuring apparatus are discussed.

If an AC voltage is applied to the electrode system of a diode consisting of a hot cathode and an anode, current will flow mainly during that part of the period in which the anode is positive with respect to the cathode. Use can be made of this rectifying action in a very simple way to measure AC voltages. It is only necessary to introduce into the anode circuit a condenser with a large resistance in parallel (see *fig. 1*). The condenser is charged by the rectified current in the circuit, while at the same time it is discharged by the resistance R. As the voltage V_c on the condenser increases, the discharging current becomes greater and the charging current smaller (see *fig. 2*). Finally the discharging current becomes equal to the average charging current so that the voltage no longer increases.

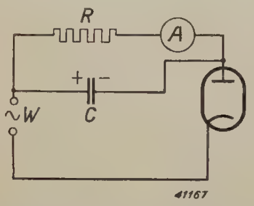

Fig. 1. Diagram showing the principle of the measurement of AC voltages by means of a diode.

The stationary value of the DC voltage V_c thus obtained forms a measure of the amplitude W of the AC voltage. The relation between W and V_c is practically independent of the frequency, provided the latter is so high that the condenser loses only little voltage in the time interval between two maxima of the intermittent charging current ($\omega CR \gg 1$). The diode is therefore a suitable device for measuring AC voltages of high frequency. To do this one simply measures the DC voltage on the condenser, or, what amounts to the same thing, the DC current through the resistance.

We shall not at this point go deeply into the relation between W and V_c, since this relation will in practice be determined experimentally [1]). We shall state only that at very small amplitudes of the AC voltage ($W < 0.1$ V) the DC voltage is proportional to W^2, while for very large amplitudes a linear relation is found between W and V_c.

At the frequencies of broadcasting waves and even in the television region (about 7 m) the calibration of the measuring arrangement performed at low frequencies will usually still hold satisfactorily. At shorter waves, however, deviations are observed which may be ascribed to the same phenomena which also hamper the use of amplifier valves in this frequency region. These phenomena, which have repeatedly been dealt with in this periodical [2]), fall into two groups: firstly the influence of undesired impedances, mainly self-induction of connecting wires and mutual capacity of electrodes, secondly inertia phenomena in the electronic valve due to the transit time of the electrons between cathode and anode. The first phenomenon results in the fact that at high frequencies a different voltage acts between cathode and anode of the valve than would be expected on the basis of the diagram of the connections as drawn. The result of this is a deviation of the diode current and thus also of the final state of equilibrium from that expected, even if it were permissible to assume that the relation between anode current and anode voltage at

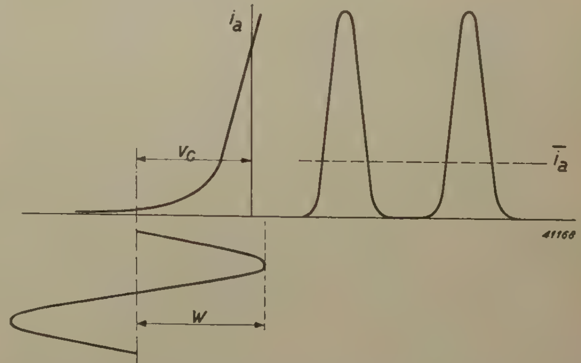

Fig. 2. If an AC voltage W with respect to the cathode acts upon the diode, the anode current i_a flows. The anode DC voltage V_c takes on such a value that the average anode current $\bar{i}_a$ is equal to the current which flows through the resistance R as a result of this voltage V_c.

---

[1]) A simplified theoretical treatment of the relation between W and Vc can be found in Philips Techn. Rev. **6**, 285, 1941.

[2]) Philips Techn. Rev. **1**, 161, 1936; **3**, 103, 1938.

these high frequencies were still given by the static characteristic.

The second phenomenon, the inertia of the electrons, results in the fact that the average anode current at very high frequencies becomes less than is calculated from the static characteristic. Part of the electrons which leave the cathode during the time when the anode is positive no longer have time to reach the anode, but when part of the way across are driven back to the cathode by the anode, which in the meantime has become negative. In *fig. 3* the behaviour of the anode current resulting from this is reproduced; for an explanation see the text under the figure.

The practical significance of these phenomena will be further explained later on in this article on the basis of apparatus actually constructed.

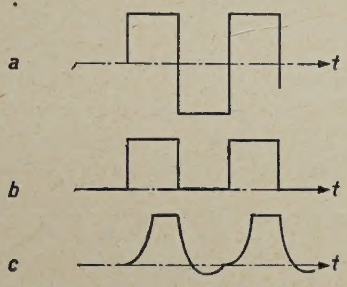

Fig. 3. Effect of the transit time of the electrons on the behaviour of the anode current.

a) Form of the anode voltage.

b) Form of the anode current when a current flows only at positive voltage.

c) Deformation of the anode current with a relatively long transit time of the electrons. The current, which is given by the number and average velocity of all the electrons present between cathode and anode, increases gradually to the stationary value after the commutation to the positive voltage, and after reversal of the voltage it decreases gradually to zero. At this point a negative current occurs temporarily due to returning electrons.

A new diode suitable for the measurement of voltages on decimetre waves

In order to be able to carry out voltage measurements in the frequency region of decimetre waves a diode was designed in this laboratory in which the disturbing factors above mentioned are avoided as well as possible. A common device for combating the effects of inertia is to diminish the distance between cathode and anode. Decreasing the distance between two electrodes, however, involves an increase in their mutual capacity. Since the capacity between cathode and anode forms one of the above-mentioned undesired circuit elements, its enlargement must be avoided. To do this it is necessary to decrease the surface of the electrodes with their distance apart. This of course means a decrease in the anode current. The limit of what can be attained in this direction is then found to be determined by the sensitivity of the available current meter.

It is obvious that full advantage can only be taken of the small dimensions of the electrode system when the connection wires to the electrodes are also kept as short as possible. Making the connection wires short is important not only to combat undesired impedances, but also to limit the external dimensions of the whole system. The momentary value of an AC voltage between two points is a well defined quantity only when the work necessary for the transportation of the unit of charge from one point to another is independent of the distance covered by the charge between the two points. In an electrostatic field this condition is always satisfied. In a high-frequency AC field, however, this is only the case when the available paths are short compared with a quarter wave length. If correct results are still required at a wave length of 50 cm, the external dimensions of the valve are limited to about 2 cm by this requirement.

The construction of the measuring diode

The measuring diode is shown in *fig. 4*. The system is mounted on a ring-shaped flange by means of which the base and the cover of the valve are fused together. The length of the connecting wires could be kept shorter than 1 cm in this way, while the dimensions of the electrode system amount to only a few millimetres.

As cathode a tungsten wire is used lying along the axis of the cylindrical anode. The cylindrical shape has a favourable effect on the transit times: the transit time between a wire and a cylinder is slightly less than that between two parallel plates the same distance apart. Moreover, the relatively high temperature of this hot cathode has the advantage that the electron shave a relatively high initial velocity, whereby the transit times are further decreased.

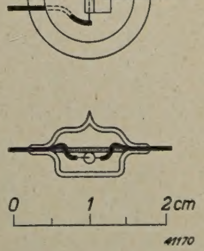

Fig. 4. Sketch of the measuring diode (external dimensions in actual size).

Results

In order to study quantitatively the influence of the various structural devices we shall consider the equivalent circuit given in *fig. 5*.

The connecting wires of cathode and anode have a certain resistance r which may be neglected at low frequencies but due to skin effect at the frequencies of decimetre waves may increase to such a degree that a disturbing damping occurs. Of still greater importance than this ohmic resistance of the wires, however, is the inductive resistance ωL, while finally the above-mentioned capacity c between cathode and anode must be taken into account.

At the frequencies of broadcasting waves and metre waves practically the entire externally applied voltage V acts on this capacity. At still higher frequencies, however, deviations begin to occur. The first phenomenon to be observed is a series resonance of the circuit L-c-L, which may cause the voltage V' on the condenser to become many times as high as the externally applied voltage V. For the resonance frequency an infinite voltage would even occur if there were no damping (resistances r and R_d) present in the circuit. If the resonance frequency is exceeded the voltage between cathode and anode rapidly falls to zero (with constant voltage between the external terminals). It is therefore only the region below the resonance frequency which has practical utility.

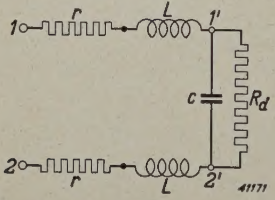

Fig. 5. Equivalent diagram of the parasitic impedances of the measuring diode which begin to exhibit an effect on the results of measurements at very high frequencies. r series resistance, L self-induction of the connection wires, c capacity between cathode and anode, R_d damping resistance caused by the transit of electrons.

The ratio V'/V is given in *fig. 6* for the new diode as a function of the frequency. For the sake of comparison corresponding curves are given for an older measuring diode and two other modern diodes. The values of L and c with which these curves are calculated are given in the following table [3]).

Table I

Selfi-nduction L of each conducting wire, capacity c between cathode and anode, and resonance frequency $f = 1/(2\pi\sqrt{2Lc})$ for the new measuring diode DA 50 compared with three other diodes designed earlier.

	L (10^{-8} henry)	c (pF)	f (10^8 c/sec)	$\lambda = 3\times10^8/f$ (m)
1) E A B	5	1,5	3,5	0,86
2) E A 50	1.8	2.1	5.8	0.52
3) Measuring diode 4674	1.5	1.65	7.1	0.42
4) Measuring diodeDA 50	0.75	0.24	26.5	0.11

As the table shows, the improvement compared with earlier diodes is quite considerable. The resonance wavelength of the new diode lies at about 11 cm, which means that the error remains less than 10 percent to a wavelength of about 30 cm. In the case of the earlier measuring diodes this limit often lies above 1 m; it may therefore be said that of voltage measurements in the decimetre wave region have only been made possible by the new construction.

When the source of the voltage to be measured has a high internal resistance, as is for example the case with a resonance circuit in tuning, errors in measurement may occur due to the damping effect of the diode connections. It is

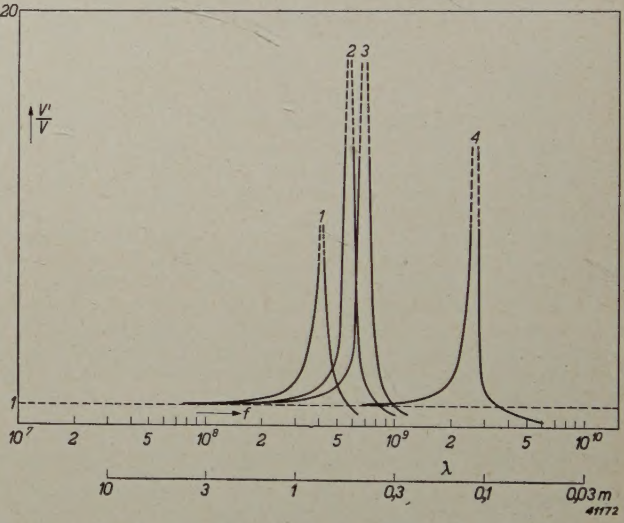

Fig. 6. Ratio of the voltage V' between cathode and anode of a diode to the voltage V between the external connection terminals of the supply wires as a function of the frequency. The variation is drawn for the equivalent circuit given in fig. 5. Curves *1* to *4* refer to the following diodes:
1) E A B, *2*) E A 50, *3*) 4674, *4*) DA 50 (new measuring diode).

---

[3]) It may be noted that the diode is often used as a relative meter to compare two voltages of the same frequency. In that case resonance phenomena of the parasitic impedances have no effect on the results of the measurement, since they have the same value in both cases. Errors may, however, occur due to the transit times of the electrons. The effect of the transit time depends not only on the frequency but also on the amplitude of the voltage applied. Nevertheless, under all practical conditions these errors remain small.

obvious that in the construction of the diode care has been taken to obtain as little damping as possible due to dielectric losses and leakages between the electrodes. Another property of the new diode which is favourable for the attenuating resistance is the extraordinary small anode current. The limitation of the anode current, which had to be accepted in order to be able to make the dimensions sufficiently small, although *per se* undesirable, is found to be an advantage in this connection. In the finished valve the average anode current in the operating region amounts to less than 1 μA; the diode has an internal resistance (attenuation resistance) of the order of 10^5 Ω. This resistance is sufficiently high for all practical cases.

At very high frequencies, as already stated, a further damping occurs as a consequence of the ohmic resistance of the connecting wires. If this attenuation is not expressed by a series resistance r, but by a new resistance R'_d in parallel between cathode and anode, the following is found:

$$\frac{1}{R_d'} = \frac{2r\ \omega^2 c^2}{(1-2\omega^2 Lc)^2}\ .$$

Since in the new measuring diode the capacity c is unusually low (see table I), the attenuation $1/R'_d$ will also remain relatively low. In order to decrease this damping still further the resistance r was decreased by using lead wire for the connections (due to the skin effect it is only the outermost layer of the wire which determines the conductivity at high frequencies). In this way R'_d is made to amount to about 10^4 Ω at a wavelength of 40 cm, which may be considered very satisfactory.

A final cause of attenuation is formed by the transit time of the electrons between cathode and anode. Due to the low value of the anode current, however, this effect remains small and may be disregarded.

The other effect of the transit time of the electrons already discussed above, the decrease in the anode current at high frequencies, is also not disturbing and to a certain extent even an advantage. Due to this the increase in the sensitivity in the region before the resonance is partially compensated, so that the characteristic remains flat over still wider frequency regions than would otherwise be the case. The dimensions of the diode are so chosen that the rise in sensitivity due to resonance begins at about the same frequency as the fall in frequency due to transit time effects. In the earlier types the resonance frequency usually lies much lower, while the transit times do not vary appreciably. This compensation phenomenon was therefore previously not taken advantage of.

Application of the diode

It would lead us too far if we were to discuss the different possibilities of connection of the diode in detail. All connections may be considered as variations of the simple principle indicated in fig. 1. These variations depend chiefly upon the varying character of the sources of voltage to be measured. The high-frequency source of voltage may possess an infinitely high resistance for direct current or it may form a short circuit; the voltage source may be earthed at one end or in the middle; all these cases require slightly different arrangements of the connections. The points of difference, however, are very obvious and involve no fundamental principles.

Of greater interest than the connection is the technical construction of the elements which are used in it. We shall here briefly discuss three of these elements: the supply line for the voltage, the valve holder and the measuring instrument. When working with very high frequencies the supply line for the voltage will often be in the form of a Lecher system on which the connection terminals of the measuring diode form sliding contacts. This principle with which the voltage can be measured as a function of the position has the advantage that there is no uncertainty about the phase of any possible standing waves at the position of the measuring diode, provided the distance between the Lecher wires is small compared with a quarter wavelength. In *fig. 7* this arrangement is shown diagrammatically; it is also evident from this figure how the cathode can be heated without the necessity of introducing disturbing extra wires in the neighbourhood of the Lecher system.

In the part to the left of the shield K only DC voltages occur. In that part the operations necessary for the measurement can be performed with outfear of any reaction on the happenings in the high-frequency part.

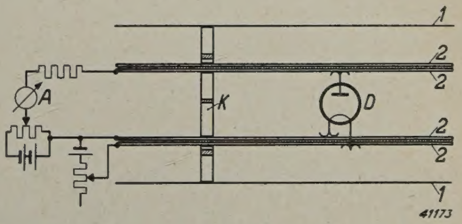

Fig. 7. Lecher system for measuring high-frequency AC voltages. *1*) external shielding, *2*) Lecher wires, K sliding bridge forming shield at the same time, D diode. Each of the wires of the Lecher system consists of two conductors separated by a layer of insulation. This division makes it possible to supply the voltage for heating the cathode *via* the Lecher system as well. Shaded parts consist of insulation material.

In the construction of the valve holder special care must be taken that the advantage of the low capacity between cathode and anode (0.24 $\mu\mu F$) is not destroyed by parasitic capacities. As few metal parts as possible will therefore be used and for the non-metallic parts a material with a low dielectric constant and as small dielectric losses as possible. In *fig. 8* a sketch is given of a valve holder constructed on this principle ; it is made of polystyrene, an artificial resin which is as clear as glass and which satisfies the requirements mentioned.

As a measuring instrument we use a reflecting galvanometer constructed in this laboratory, whose most important properties are described elsewhere in this number in connection with the discussion of a cable measuring bridge. This instrument excels by its sensitive yet sturdy system, which, in contrast to many other sensitive galvanometer systems, need not be placed in a horizontal position. Deviating from the description given on page 114, in our case a coil with an internal resistance of 500 Ω was used; moreover, in our case it was unnecessary to take special precautions for the insulation of the measuring system against high voltages. *Fig. 9a* gives a sketch of the construction of the instrument, while *fig. 9b* shows the external finish of an experimental model.

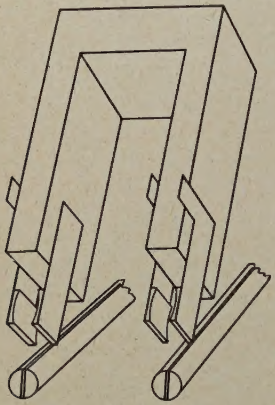

Fig. 8. Valve holder for the measuring diode. The non-metallic parts are mode of polystyrene.

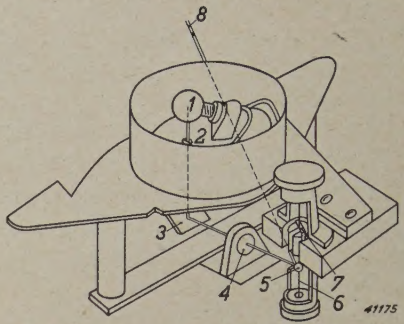

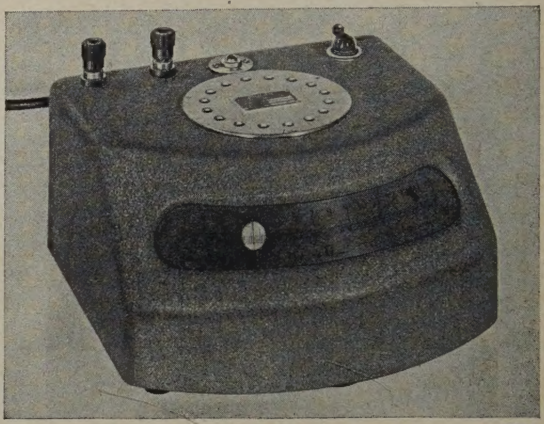

Fig. 9. *a*) Reflecting galvanometer suitable for measuring the DC of the measuring diode. *1*) lamp, *2*) diaphragm with black lines, *3*) mirror, *4*) lens which focuses the black line on the scale, *5*) rotating mirror which together with the coil *7*) is suspended between the wires *6*), *8*) beam of light toward, the scale.
b) Form of construction of the reflecting galvanometer.